Radboud University Nijmegen

Faculteit der Natuurwetenschappen, Wiskunde en Informatica

Decoupling Heavy Fermions in the Scalar Sector

Choosing an Appropriate Renormalization Scheme

Author:
S.A.W. de Wit

Supervisor:
prof dr. W.J.P. Beenakker

Department of High Energy Physics (HEP)
Institute for Mathematics, Astrophysics and Particle Physics (IMAPP)

August 24, 2022

Acknowledgements

First and foremost, I would like to express my sincere gratitude to my supervisor prof. dr. Wim Beenakker. First of all, his extensive knowledge on quantum field theory combined with his calm and clear method of explaining complicated subjects provided invaluable guidance during my internship. Furthermore it has been an honor that he has allowed me so much of his precious time during our bi-weekly meetings. This made possible interesting and fruitful discussions about the subject of this thesis. I thoroughly enjoyed our meetings which often also included interesting conversations on subjects beyond those directly related to the content of this thesis. Lastly I have to mention prof. dr. Beenakkers positive attitude during all of the meetings. It has been a pleasure to work with you, thank you.

Secondly I would like to thank prof. dr. Sijbrand de Jong for making time in his busy schedule as faculty dean to evaluate this work as the second reader.
Lastly I would like to mention my loving wife, my family and close friends. Your continuous support and much needed disctractions were of great motivational value.

Contents

1 Introduction

In the 20th century physicist Paul Dirac was the first person to successfully combine the theory of quantum mechanics (QM) with special relativity. The first quantum field theory (QFT) was born in 1927 when Dirac published his paper on quantum electrodynamics (QED) [1]. QED describes the interactions between light and matter and has produced some of the most accurate agreements between predictions and experiments. To achieve accurate theoretical predictions, calculations in QFT are performed by making use of perturbation theory. Feynman diagrams were introduced as pictorial representations of scattering processes to be calculated [2]. These diagrams provide a comprehensible method to determine which terms in the series expansion are to be included. Each Feynman diagram corresponds to a mathematical expression. From the specific theory the Feynman rules for the diagrams can be derived, which help to 'translate' the diagrams to mathematical expressions. Interactions between particles are described by the exchange of (virtual) gauge bosons. In the case of QED the gauge boson is the photon. The theory of QED came with some theoretical challenges. The most striking one was the appearance of infinities in the calculations. The lowest order calculation gave a good approximation for a measured quantity. However, more precise calculations were needed as experiments became more and more accurate. In terms of Feynman diagrams this translates to taking into account diagrams that have internal loops, which will often lead to infinities. Between 1947 and 1949 Feynman, Schwinger and Tomonaga developed the groundwork to deal with these infinities, for which they received the Nobel prize in 1965 [3].

Nowadays the world of particle physics is described by a number of QFT's which are summarized in the Standard Model (SM) of particle physics. This combined theory describes not only the electromagnetic force but also the weak and strong interactions. For the development of the latter theories more intricate mathematical machinery was required. The emergence of the theory of the weak interactions brought along new challenges; for the first time the gauge bosons were massive. Gauge invariance of the theory does not allow for massive gauge bosons. The problem was solved by Peter Higgs along with five others in 1964 [4]. The solution brought along a new particle; the famous Higgs boson which was experimentally discovered in 2012 at CERN [5].

Self-energy diagrams describe the change that the mass of a particle undergoes due to self-interactions. These quantum corrections on the mass of a particle cause the observed mass to be different from the bare mass present in the Lagrangian. These corrections apply to all particles in the SM, but give rise to complications in the case of the Higgs boson. This particle is exceedingly sensitive to corrections by heavy particles. For particles in the SM the corrections do not cause issues. The trouble appears when considering the possibility of heavier (undiscovered) particles. These particles participate in the virtual loops of self-energy calculations. The Higgs boson receives corrections that are quadratically dependent of the mass of these heavy particles. The fact that we observe a (relatively) light Higgs boson requires a huge amount of fine-tuning.

This thesis is a succession to the thesis by Guus Reijns, who investigated self-energy corrections to the Higgs mass [6]. He concludes that the dependence of the self-energy on the mass of the heavy particle depends on the renormalization scheme that is used. In this work we will further investigate the influence of a renormalization scheme on the (non-)decoupling properties of amplitudes. In section 2 some basic QFT concepts that are relevant throughout this work will be discussed. This section will start with the formulation of QED, which will also be the working example for various concepts that are discussed later. The origin of particle masses in the SM will be explored in section 2.2. The methods for dealing with infinities in calculations are touched upon in section 2.3 and 2.4.

In section 3 the Appelquist-Carazzone decoupling theorem will be explored and proven for a specific gauge theory. Thereafter, in section 4 a scalar toy model will be constructed as a means to examine decoupling properties of the scalar sector. In the first few sections of this thesis, calculations will be fairly detailed. As we go further, more details will be left out, but full calculations can be found in appendix E.

1.1 Conventions

The Einstein summation convention will be used throughout this work. This states that summation is implied over repeated indices. For example, the square of a four-vector is written as:

$$x^2 \equiv \sum_{\mu} x_\mu x^\mu = \sum_{\mu,\nu} g_{\mu\nu} x^\mu x^\nu = g_{\mu\nu} x^\mu x^\nu \ , \tag{1.1}$$

where the last step shows the Einstein summation convention explicitly.
Natural units will be used for the entirety of this work i.e.:

$$\hbar = c = \epsilon_0 = 1 \ , \tag{1.2}$$

unless explicitly stated otherwise. The following convention for the Minkowski metric $g^{\mu\nu}$ will be used:

$$g^{\mu\nu} = \begin{pmatrix} 1 & 0 & 0 & 0 \\ 0 & -1 & 0 & 0 \\ 0 & 0 & -1 & 0 \\ 0 & 0 & 0 & -1 \end{pmatrix} \ . \tag{1.3}$$

In this work, calculations often involve fermionic interactions. These will introduce the set of Dirac matrices, whose defining property is:

$$\{\gamma^\mu, \gamma^\nu\} = \gamma^\mu \gamma^\nu + \gamma^\nu \gamma^\mu = 2g^{\mu\nu} \mathbb{1} \ , \tag{1.4}$$

where $\mathbb{1}$ is the identity matrix. We will mostly work without an explicit representation of these matrices.[1] An explicit representation that is often used is the Weyl representation:

$$\gamma^0 = \begin{pmatrix} 0 & \mathbb{1}_2 \\ \mathbb{1}_2 & 0 \end{pmatrix}, \quad \gamma^k = \begin{pmatrix} 0 & \sigma^k \\ -\sigma^k & 0 \end{pmatrix}, \quad \gamma^5 = \begin{pmatrix} -\mathbb{1}_2 & 0 \\ 0 & \mathbb{1}_2 \end{pmatrix} \ . \tag{1.5}$$

In this equation the index $k = 1, 2, 3$, σ^k are the 2 x 2 Pauli spin matrices (see appendix D.2) and $\mathbb{1}_2$ is the 2 x 2 identity matrix. Note that, in this representation, the gamma matrices are all 4×4 matrices, which is the lowest possible dimension for which a representation satisfying equation 1.4 can be constructed. Furthermore, $\gamma^5 \equiv i\gamma^0\gamma^1\gamma^2\gamma^3$ is a useful combination of gamma matrices.[2]
In this work, we'll deal with three types of fields. Scalar fields (spin 0) are denoted by ϕ, fermionic fields (spin 1/2) are denoted by ψ and their adjoint field by $\bar{\psi}$.[3] Gauge boson fields (spin 1) will be indicated by A^μ.

[1] The result of a calculation is independent of the representation, as it should be.
[2] The 5 is an index, so γ^5 does not mean some γ raised to the fifth power.
[3] The adjoint field is defined by $\bar{\psi}(x) \equiv \psi^\dagger(x)\gamma^0$ where the † indicates Hermitian conjugation.

2 Theory

In this section, some relevant subjects of Quantum Field Theory will be discussed.

2.1 Gauge invariance

First, the concept of gauge invariance will be explored, starting with the Lagrangian[4] of Quantum Electrodynamics (QED) and its symmetries. Subsequently the idea of symmetries will be extended to a wider class of Lagrangians, while the viewpoint of what is fundamental will switch. After discussing the QED lagrangian, a consequence of the gauge symmetry will be revealed; the Ward-Takahashi identity. Thereafter the discussion will be extended to the case of non-Abelian theories.

2.1.1 Quantum Electrodynamics

The QED Lagrangian can be constructed in two (similar) ways. Firstly, one can begin with the lagrangian of Dirac fermions with charge $|e|$ in an electromagnetic field and apply minimal substitution ($p^\mu \to p^\mu - |e|A^\mu$) followed by the quantum substitution of observables by operators (effectively replacing: $i\partial^\mu \to i\partial^\mu - |e|A^\mu$). In these equations A^μ is the electromagnetic four-potential. After this the kinetic term is added ($\mathcal{L}_{Maxwell}(x) = -1/4F_{\mu\nu}(x)F^{\mu\nu}(x)$) resulting in the QED Lagrangian:

$$\mathcal{L}_{QED}(x) = \bar{\psi}(x)(i\partial\!\!\!/ - m)\psi - 1/4F_{\mu\nu}(x)F^{\mu\nu}(x) - |e|\bar{\psi}(x)\gamma^\mu\psi(x)A_\mu(x). \tag{2.1}$$

Here $F^{\mu\nu}(x)$ is the field strength tensor for the gauge field, which is given by:

$$F_{\mu\nu}(x) \equiv \partial_\mu A_\nu(x) - \partial_\nu A_\mu(x). \tag{2.2}$$

Alternatively, one can begin with the free Dirac Lagrangian as a starting point:

$$\mathcal{L}_{Dirac}(x) = i\bar{\psi}(x)\gamma^\mu\partial_\mu\psi(x) - m\bar{\psi}(x)\psi(x). \tag{2.3}$$

One can easily check that this Lagrangian is invariant under the global U(1) gauge transformation:

$$\begin{aligned} \psi(x) &\to \psi'(x) = e^{i\alpha}\psi(x) \ , \\ \bar{\psi}(x) &\to \bar{\psi}'(x) = e^{-i\alpha}\bar{\psi}(x) \ , \end{aligned} \tag{2.4}$$

where α is a real number, independent of the spacetime coordinate x^μ. Next, the gauge principle will be invoked. The gauge principle states that the global gauge invariance should also hold for local transformations:

$$\begin{aligned} \psi(x) &\to \psi'(x) = e^{i\alpha(x)}\psi(x) \ , \\ \bar{\psi}(x) &\to \bar{\psi}'(x) = e^{-i\alpha(x)}\bar{\psi}(x) \ . \end{aligned} \tag{2.5}$$

If we now check this requirement for the Dirac Lagrangian 2.3, we see that local gauge invariance is satisfied for the mass term, but not for the kinetic term. To also make this term invariant, the derivative ∂_μ is replaced by a covariant derivative D_μ:

$$D_\mu \equiv \partial_\mu + i|e|A_\mu(x) \ , \tag{2.6}$$

[4] Note that, strictly speaking, what is called a Lagrangian here is actually a Lagrangian density. The Lagrangian is the spatial integral over the Lagrangian density.

where the gauge field A_μ transforms according to:

$$A_\mu(x) \to A'_\mu(x) = A_\mu(x) - \frac{1}{|e|}\partial_\mu \alpha(x) \ . \tag{2.7}$$

It is now straightforward to check that the following Lagrangian is locally gauge invariant:

$$\begin{aligned}\mathcal{L}(x) &= i\bar{\psi}(x)\gamma^\mu D_\mu \psi(x) - m\bar{\psi}(x)\psi(x) \\ &= i\bar{\psi}(x)\gamma^\mu \partial_\mu \psi(x) - m\bar{\psi}(x)\psi(x) - |e|\bar{\psi}(x)\gamma^\mu \psi(x) A_\mu(x) \ .\end{aligned} \tag{2.8}$$

It contains the free Dirac Lagrangian and an (gauge) interaction term:

$$\mathcal{L}_{int}(x) = -|e|\bar{\psi}(x)\gamma^\mu \psi(x) A_\mu(x) \ . \tag{2.9}$$

There are two important things to notice at this point. First of all, we see that we can scale the interaction strength by scaling the coupling e (which in QED is the charge of the particle). This is done by writing the charge as $q = Q|e|$, modifying the gauge transformation as $\exp(i\alpha(x)) \to \exp(iQ\alpha(x))$ and the gauge coupling as $|e| \to Q|e|$ which changes the covariant derivative as $D_\mu \to \partial_\mu + iQ|e|A_\mu$. The transformation of the gauge field is unaffected, but the interaction strength is now q instead of $|e|$. The original QED theory is formulated for electrons for which q=-|e|=e.
Second of all, we *need* the introduced gauge field to be massless. If we would have a mass term for the gauge field in our Lagrangian ($\frac{1}{2}M_A^2 A_\mu(x)A^\mu(x)$), the Lagrangian would no longer be gauge invariant as a result of equation 2.7. Luckily, in QED the gauge boson is the photon, which *is* massless. However, in gauge theories that contain massive gauge bosons, these cannot simply be added 'by hand', hence another way of adding these mass terms is needed.
To complete the QED lagrangian, the gauge invariant kinetic term $-1/4F_{\mu\nu}(x)F^{\mu\nu}(x)$ is added, where:

$$iqF_{\mu\nu} \equiv [D_\mu, D_\nu] \ . \tag{2.10}$$

The Feynman rules for QED can be derived from the resulting Lagrangian. These are summarized in appendix C.

The Ward identity

From the form of the QED Lagrangian, conservation of electric charge can be proven. This follows from applying Noether's theorem[5] to the symmetries in the Lagrangian (see for example [7] or [8]). The resulting conserved currents give rise to Ward identities[9]. The Ward identity applies to matrix elements calculated (in momentum space) with one or more external photons (or other massless gauge-bosons). Let this matrix element be denoted by $\mathcal{M}$ and k be the four momentum carried by the external photon under consideration. We can then write:

$$\mathcal{M}(k) = \epsilon_\mu(k)\mathcal{M}^\mu(k) \ , \tag{2.11}$$

where $\epsilon_\mu(k)$ is the polarization vector of the photon and $\mathcal{M}^\mu$ is the part of the amplitude to which the the photon attaches. The Ward identity states that, if we replace the photon polarization vector by the momentum vector, the resulting expression evaluates to 0:

$$k_\mu \mathcal{M}^\mu(k) = 0 \ . \tag{2.12}$$

[5] Noether's theorem states that, every continuous symmetry in a theory has a corresponding conservation law.

This relation is also directly related to the fact that (massless) gauge bosons do not have a longitudinal polarization.[6] Actually the Ward identity also applies to internal (virtual) photons. So, there is no need for $k^2 = 0$ to hold. The Ward identity has some useful consequences, one of which we'll use in section 2.2.3 to simplify the tensor structure of a matrix element.

2.1.2 Non-Abelian Gauge invariance

In the last section, the QED lagrangian was found in two different ways. The second method makes use of the idea that the found local gauge invariance is not just a coincidence of the theory. It in fact *is* the fundamental principle that determines the form of the Lagrangian. In this viewpoint, the very existence of the gauge field is a consequence of the local symmetry. It is needed to write an invariant Lagrangian containing derivatives of the fields ψ. This idea can be generalized to invariance of Lagrangians under any local symmetry group. To this end, instead of considering a single Dirac field, a doublet of Dirac fields is considered:

$$\psi = \begin{pmatrix} \psi_1(x) \\ \psi_2(x) \end{pmatrix} \ ,$$

that transforms under three-dimensional rotations as:

$$\psi \to \exp\left(i\alpha^j \frac{\sigma^j}{2}\right)\psi \ . \tag{2.13}$$

The σ^j ($j = 1, 2, 3$) are the Pauli spin matrices, and the Einstein summation convention implies summations over the repeated index j. Next, the gauge principle is invoked, by requiring that the Lagrangian is invariant under the transformation 2.13 where α^j is an arbitrary function of x. This is more involved than the U(1) case discussed before, because there are now three orthogonal symmetry possibilities that do not commute with each other. Field theories with these noncommuting local symmetries are called non-Abelian gauge theories. Following the same procedure as before, a covariant derivative is required, e.g. for local SU(2)[7] symmetry:

$$D_\mu \equiv \partial_\mu - igA_\mu^j \frac{\sigma^j}{2} \ . \tag{2.14}$$

Here, g is the gauge coupling and three gauge fields are required. Due to the non-commutativity, the field strength tensor is no longer gauge invariant. This can be seen from working out the commutation relations of the Pauli spin matrices, so that

$$F_{\mu\nu}^i = \partial_\mu A_\nu^i - \partial_\nu A_\mu^i + g\epsilon^{ijk} A_\mu^j A_\nu^k \ . \tag{2.15}$$

The last term in this expression was absent in the U(1) case. Even though the field strength tensor itself is not gauge invariant, it is still possible to write gauge invariant combinations like the Yang-Mills (YM) Lagrangian:

$$\mathcal{L}_{YM} = -\frac{1}{2}\,\mathrm{Tr}\left\{(F_{\mu\nu}^i \frac{\sigma^i}{2})^2\right\} = -\frac{1}{4}(F_{\mu\nu}^i)^2 \ . \tag{2.16}$$

Using this, we can construct the SU(2) Lagrangian, which describes the simplest non-Abelian gauge theory:

$$\mathcal{L}_{SU(2)} = \bar{\psi}(i\not{D})\psi - \frac{1}{4}(F_{\mu\nu}^i)^2 - m\bar{\psi}\psi \ . \tag{2.17}$$

[6]We can be a bit more careful with our wording: longitudinal polarizations of massless bosons do not show up in matrix elements.

[7]SU(N) is the special unitary group of degree N. It is the Lie group of $N \times N$ unitary matrices with determinant 1. For more background, see appendix D.3.

The extra term in the field strength tensor is the origin of gauge boson self interactions in Quantum Chromo-Dynamics (QCD) and the weak interactions. This term is absent in the case of QED, and the photon does not couple to itself.[8] The methods described above can be further generalized to larger symmetry groups. The SM is built from the local symmetry groups $SU(3)_C \times SU(2)_L \times U(1)_Y$.
The L in $SU(2)_L$ stands for 'left-handed', indicating that the SM is a chiral theory. In a chiral theory left- and right-handed fields are treated differently. A spinor can be composed in its left- and right-handed states by using projection operators:[9]

$$\begin{aligned} \psi_L \equiv P_L \psi = \frac{1}{2}(\mathbb{1} - \gamma^5)\psi \ , \\ \psi_R \equiv P_R \psi = \frac{1}{2}(\mathbb{1} + \gamma^5)\psi \ , \end{aligned} \tag{2.18}$$

where $\mathbb{1}$ indicates the identity matrix in four dimensions. The group $SU(2)_L$ has the quantum number I, called weak isospin, associated with it. The third component of weak isospin (I_3) runs from $-I$ to $+I$, so a field that has weak isospin I is a (2I+1)-dimensional multiplet. In the weak, electromagnetic and strong interactions, I_3 is conserved.
The Y in $U(1)_Y$ stands for (weak) hypercharge. Weak hypercharge is related to the electric charge Q by[10] $Q = I_3 + Y/2$.
Lastly, the C in $SU(3)_C$ stands for color. The $SU(3)_C$ group acts on colored fermions; quarks are the only fermions that carry color. There are three possible values for the color charge: red, green and blue. The bosons associated with this force are the gluons.
As in the case of QED, if gauge invariance is to be preserved, it is not possible to add a mass term for the gauge bosons to the Lagrangian. In the case of the photon and the gluons this is not an issue, but in the case of the weak interactions, the gauge bosons ($W^\pm$ and Z^0) are known to be massive (80 and 91 GeV respectively [10]). An alternative method to give mass to these bosons is needed, which will be discussed in section 2.2.2.

2.2 Mass in the Standard Model

In this section the origin of mass in QFT and the SM will be discussed. The problem with masses of fermions and bosons will be debated as well as the solution to this problem; the Higgs mechanism. As stated before, in QED there is no 'problem' with masses. The massive fermions in this theory are not chiral and the photon is massless. Problems arise when we look at the electroweak sector of the SM, where there is a differentiation between left- and-right-handed particles and the bosons are massive.

2.2.1 Mass parameters and invariance

Before going into the possible problems with mass terms, let us first recall that the terms in the Lagrangian that are quadratic in the fields and do not involve derivatives are identified as mass terms. The Feynman rules for a given theory follow from the Lagrangian and the mass of a particle shows up as the pole of the propagator (see for example the electron propagator in appendix C).
As stated in the last section, we require the Lagrangian to be gauge invariant. Now consider the case where we do have a chiral theory. We can decompose the mass term in the Lagrangian by using the projections of

[8] Thinking more diagrammatically; the photon couples to particles with (electric) charge, but is not charged itself. In contrast, gluons couple to color charge and carry color themselves.
[9] A projection operator P has the property that the effect of applying it twice is the same as applying it once.
[10] This relation is called the Gell-Mann Nishijima relation.

the field given in equation 2.18:

$$-m\bar{\psi}\psi = -m(\bar{\psi}_L\psi_R + \psi_L\bar{\psi}_R)\ . \tag{2.19}$$

Because the L/R-handed fields are treated differently in a chiral theory, the mass term in the Lagrangian is not gauge invariant. An alternative method to introduce mass terms is needed, rather than adding them 'by hand'. This is the case in the SM, where in the electroweak sector left-handed fields do transform under $SU(2)_L$, whereas right-handed fields do not.

The problem with mass terms for the bosons, touched upon in section 2.1.1, is less relevant in the context of this thesis. Nevertheless if one has a theory with massive gauge bosons, one also needs a way to give them mass. To this end, we want to 'break gauge invariance, without actually breaking it'.

2.2.2 The Higgs mechanism

In 1964 Peter Higgs along with five other theorists managed to solve the problem of giving mass to particles without breaking gauge invariance. The solution introduces the concept of spontaneous symmetry breaking (SSB)[4][11]. The basic idea is that a mass term can actually be 'hidden' in a Lagrangian, where it is only revealed when the Lagrangian is rewritten. To illustrate the idea behind the Higgs mechanism, we'll use an example in a simple setting. As before, we'll use QED as the working example. In QED the gauge boson (the photon) is massless, but imagine for a moment that we would have experimental evidence that the photon is not massless. We would like to have a QED theory with a massive gauge boson. The mass term cannot simply be added to the Lagrangian, as discussed in section 2.1.1, as it would break gauge invariance. The solution is to add a new complex scalar[11] field ϕ to the Lagrangian as well as a potential term $-V(\phi)$. The (relevant part of the) Lagrangian looks like:

$$\mathcal{L}(x) = -\frac{1}{4}\big(F_{\mu\nu}\big)^2 + |D_\mu\phi|^2 - V(\phi)\ , \tag{2.20}$$

with the covariant derivative defined the same as in equation 2.6; $D_\mu = \partial_\mu + i|e|A_\mu$. Let the potential be:[12]

$$V(\phi) = -\chi^2\phi^*\phi + \frac{\lambda}{2}(\phi^*\phi)^2\ , \tag{2.21}$$

with $\chi^2 > 0$. We notice that the minimum of the potential is not at the origin, there actually is an unstable maximum at the origin. The minimum of the potential is at $|\phi_0| = (\frac{\chi^2}{\lambda})^{1/2}$, this is also called the vacuum expectation value (vev). Notice that there is a degenerate set of minima in the complex ϕ-plane. The 'choosing' of one of the minima in the ring causes the $U(1)$ symmetry to be spontaneously broken. The form of the potential (often referred to as the 'Mexican hat' potential) is shown in figure 1.

[11] Spin 0.

[12] In the literature μ is often used instead of χ, however throughout this work μ is already used for multiple concepts so χ is used here.

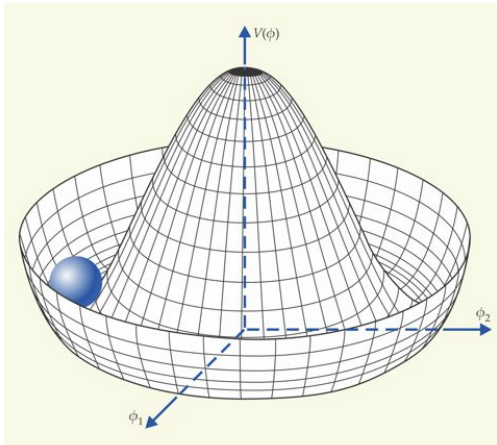

Figure 1: Higgs Potential [12].

Furthermore, we're dealing with perturbation theory, in which we start from the 'ground state'. In this approach we treat the fields as fluctuations around the ground state. So the next step is to rewrite the complex scalar field ϕ as:

$$\phi(x) = \phi_0 + \frac{1}{\sqrt{2}}(\phi_1(x) + i\phi_2(x)) \ . \tag{2.22}$$

Applying this decomposition to the potential of equation 2.21 results in:

$$V(\phi) = -\frac{\chi^4}{2\lambda} + \chi^2\phi_1^2 + \dots \ , i = 1, 2 \ , \tag{2.23}$$

where the dots indicate higher order terms in the fields. From this we see that the ϕ_1 field now has a mass of $m_1 = \sqrt{2}\chi$. The ϕ_2 field is massless and is called the *Goldstone boson*. In figure 1 the massless Goldstone boson corresponds to fluctuations in the 'flat' direction along the ring of minima. The massive field corresponds to fluctuations in the direction of the 'walls' of the potential.
Next, let us investigate what the consequence of the redefinition of the scalar field is for the kinetic term:

$$|D_\mu\phi|^2 = \frac{1}{2}(\partial\phi_1)^2 + \frac{1}{2}(\partial\phi_2)^2 + \sqrt{2}|e|\phi_0 A_\mu \partial^\mu \phi_2 + e^2\phi_0^2 A_\mu A^\mu + \dots \ , \tag{2.24}$$

where the dots indicate terms that are cubic/quartic in the fields. From the last term we see that we've achieved our goal; the photon field has gained a mass term with $m_A^2 = 2e^2\phi_0^2$. We also notice that we have a coupling between the gauge boson and the Goldstone boson. To remove the unphysical Goldstone boson from the theory, we switch to the *unitary gauge*. This gauge fixes the field ϕ in such a way that it becomes real-valued at every point. This removes the ϕ_2 field from the theory. One can argue that the Goldstone boson has not completely disappeared from the theory. Notice that a massless boson has two polarizations (both transverse). When the boson becomes massive, it gains an extra polarization which has to have come from somewhere. The extra degree of freedom (DoF) was supplied by the Goldstone boson. This is sometimes described as the Goldstone boson being 'eaten' by the gauge field.

We've seen a simplified example where we were able to give mass to the photon. In the SM it is not the photon that is massive, but the $W^\pm$ and Z^0 bosons. The process of giving mass to these particles is similar to the procedure described above. This time a complex scalar doublet of Higgs fields is introduced. The doublet has four degrees of freedom. After going through the entire procedure, three of the four bosons in the electroweak sector have gained a mass and one has remained massless. Furthermore, the theory has an extra (scalar) particle: the Higgs boson.[13] The prediction of the Higgs boson was experimentally confirmed in 2012 at the LHC at CERN. Both the ATLAS[5] and CMS[13] collaborations measured the existence of a Higgs boson with a mass of $\sim 125\ GeV$.

The Higgs mechanism can also be used to give mass to the fermions in the SM. This is done by adding Yukawa interactions to the theory. Due to SSB the Higgs has acquired a non-zero vev, giving rise to a fermionic mass term. This procedure also results in an interaction vertex between fermions and the physical Higgs boson:

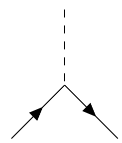

$$\leftrightarrow -i\frac{\lambda_f}{\sqrt{2}}\ , \tag{2.25}$$

where λ_f is the Yukawa coupling, which is related to the fermion mass, m_f, by: $\frac{\lambda_f}{\sqrt{2}} = \frac{m_f}{v}$. In this equation $\phi_0 = v/\sqrt{2}$ is the vev of the Higgs field.

2.2.3 Self-energy

The propagator describes how a particle propagates through spacetime; it is a time-ordered propagation amplitude associated with the transition amplitude for one spacetime state to go to another spacetime state at a later time. The Feynman rule for the electron propagator in QED is given by:

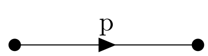

$$\leftrightarrow \quad \frac{i(\not{p} + m)}{p^2 - m^2 + i\eta}\ , \tag{2.26}$$

where the $i\eta$ is used to infinitesimally shift the pole in the complex plane to ensure that momentum integrations are well defined. In calculations in this work, the $i\eta$-term in the denominator will be implied and not written out explicitly.

The above Feynman rule is for the 'bare propagator', where no quantum corrections are taken into account. Taking into account quantum corrections to the propagator amounts to considering *self-energy diagrams*. Self-energy diagrams are loop corrections to the propagator given in terms of *one-particle irreducible* (1PI) diagrams. A Feynman diagram is 1PI if it contains no internal line that, when cut makes the diagram disconnected. At the one loop level, for electrons in QED, there is only one 1PI self-energy diagram:

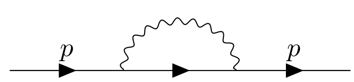

,

which is denoted by $-i\Sigma^{(1)}(\not{p})$. This can be used to calculate the one-loop correction to the propagator given by:

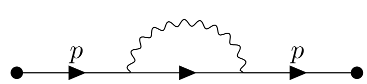

,

[13] In popular science, the Higgs boson is often called 'the God particle'. I'm not sure what percentage of physicists actually like this name.

which corresponds to

$$\frac{i(\not{p}+m)}{p^2-m^2}\big(-i\Sigma^{(1)}(\not{p})\big)\frac{i(\not{p}+m)}{p^2-m^2} = \frac{i}{\not{p}-m}\big(-i\Sigma^{(1)}(\not{p})\big)\frac{i}{\not{p}-m}\ . \tag{2.27}$$

There is now a double pole at $p^2 = m^2$. If we take into account all-order 1PI diagrams, the notation for the self-energy changes to $i\Sigma(\not{p})$. Furthermore, we can have insertions of these 1PI blobs (all possibilities) multiple times, leading to the diagrammatic equation:

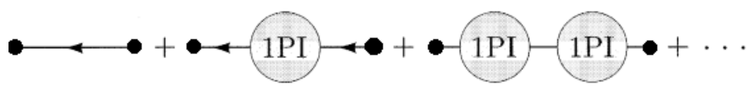

This evaluates to:

$$\frac{i}{(\not{p}-m)} + \frac{i}{(\not{p}-m)}\big(-i\Sigma(\not{p})\big)\frac{i}{(\not{p}-m)} + \ldots \tag{2.28}$$

Next, we realize that $\Sigma(\not{p})$ commutes with $\not{p}$ and use this to sum the expression through Dyson summation:

$$(2.28) = \frac{i}{\not{p}-m}\sum_{n=0}^{\infty}\Big(\frac{\Sigma(\not{p})}{\not{p}-m}\Big)^n = \frac{i}{\not{p}-m-\Sigma(\not{p})}\ , \tag{2.29}$$

where we see that we've found a new simple pole at a shifted mass. If we are to interpret the pole of the propagator as the physical mass of the particle, the original mass term in the Lagrangian[14] cannot be the mass that is measured in experiments, a fact that we'll use in section 2.4.1.

2.3 Regularization

2.3.1 Power counting

When working with Feynman diagrams involving loops, one often finds divergent integrals over the undetermined loop momentum (or loop momenta in case of diagrams involving multiple loops). Before we attempt to handle the divergences, it is useful to be able to quickly determine whether or not a diagram (or its corresponding integral) diverges, and to what extent it diverges. A useful way of determining this, is by the procedure of *naive powercounting*. This method compares the powers of momentum in the denominator and the numerator of an integral. We define the *superficial degree of divergence* D as the difference:

$$D \equiv (\text{power of k in numerator}) - (\text{power of k in denominator})\ , \tag{2.30}$$

where k indicates a momentum to be integrated over. Here all loop momenta and components of loop momenta are considered to be of the same large order of magnitude. The value of D tells us how divergent a diagram is. When $D < 0$ the diagram is convergent, when $D = 0$ the diagram is logarithmically divergent, $D = 1$ corresponds to a linear divergence, $D = 2$ to a quadratic divergence and so on.
As an example, consider the following integral:

$$I^{\mu\nu} = \int \frac{d^4k}{(2\pi)^4}\frac{k^\mu k^\nu}{(k^2-m^2)^2}\ . \tag{2.31}$$

[14]Obtained with or without the Higgs mechanism.

Here we have 6 powers of momentum in the numerator, and 4 powers of momentum in the denominator, this integral then has $D = 2$ and is considered quadratically divergent.

For a particular field theory, this degree of divergence can also be determined from a Feynman diagram, by looking at the number of loops and the powers of momentum that each propagator contributes. For example, for QED, we have:

$$D = 4L - P_e - 2P_\gamma \ , \tag{2.32}$$

where L is the number of loops in the diagram, P_e is the number of fermionic propagators and P_γ is the number of photon propagators. From the Feynman rules for the propagators (C.1) it can be seen that a fermion propagator has one power of momentum in the denominator, whereas a photon propagator has two powers of momentum in the denominator.

Consider as an example a diagram which is a correction to the QED vertex:

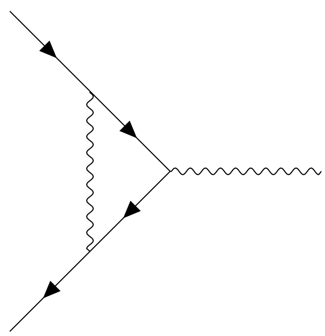

Figure 2: QED vertex correction.

According to formula 2.32 this diagram has $D = 0$ ($P_e = 2$ and $P_\gamma = 1$), which corresponds to a logarithmic divergence. This naive method of determining the degree of divergence is often wrong. Consider for example the following diagram that is part of the process $e^+e^- \to \mu^+\mu^-$

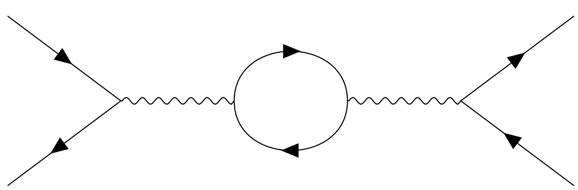

Figure 3: One loop contribution to $e^+e^- \to \mu^+\mu^-$.

This diagram has one loop, $L = 1$, $P_e = 2$ and $P_\gamma = 2$, which would lead to $D = -2$ and give rise to the conclusion that the diagram is finite. However, the diagram contains a divergent subdiagram, causing the entire diagram to be (logarithmically) divergent. Note also that the momentum in the photon propagator is independent of the loop momentum but only depends on the external momenta, hence they do not contribute to D. Lastly, note that this diagram is not 1PI; the photon lines are reducible.
We can consider the subdiagram of this:

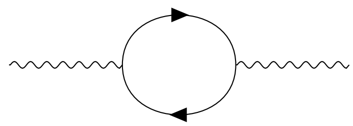

Figure 4: Photon self-energy diagram.

This diagram has $D = 2$ but is only logarithmically divergent, this is due to the aforementioned Ward-identity.
Lastly, there is the diagram with one external photon. Diagrams like these are called *tadpole diagrams*. The tadpole diagram in QED vanishes because of charge conjugation invariance[15]. If we evaluate the tadpole diagram, it is proportional to the electromagnetic current operator[16] which changes sign upon charge conjugation. Under charge conjugation the diagram evaluates to minus itself, hence it has to be zero.
To conclude; the superficial degree of divergence is a useful tool in characterizing 'how divergent' a particular diagram is, but the method has to be used with care. We will come back to this explicitly.
Equation 2.32 can be rewritten to depend less on the internal structure of the diagram. To this end, let us look at the amount of loops in a diagram:

$$L = P_e + P_\gamma - V + 1 \ . \tag{2.33}$$

This equation is found by realizing that each loop results in an overall undetermined momentum to be integrated over, so counting the amount of loop integrations is equal to counting the amount of undetermined momenta. Each propagator introduces one momentum integral, whereas momentum conservation is imposed at each vertex (i.e. each vertex introduces a delta function) and one delta function is used for overall momentum conservation.
Next, the number of vertices can be determined by looking at the amount of lines connected to the vertices:

$$V = 2P_\gamma + N_\gamma = \frac{1}{2}(2P_e + N_e) \ , \tag{2.34}$$

where N_i indicates external lines of type i. Note that the internal lines count twice, because they are connected to two vertices. Note also that the factor 1/2 comes from the fact that each vertex is connected to *two* electron lines and only one photon line. These expressions can be substituted into equation 2.32 to find:

$$D = 4 - N_\gamma - \frac{3}{2}N_e \ . \tag{2.35}$$

This expression tells us that QED only has a finite number of (superficially) divergent amplitudes: those where the amount of external legs is not too large. Note also that the degree of divergence is independent of the amount of vertices V, so divergences occur at all orders in perturbation theory. Such a theory is called *renormalizable*. The term renormalizable stems from the fact that there a finite amount of divergencies to deal with.

If we extend the previous reasoning to an arbitrary number of spacetime dimensions d, the result for QED would be:

$$D = dL - P_e - 2P_\gamma = d + \big(\frac{d-4}{2}\big)V - \big(\frac{d-2}{2}\big)N_\gamma - \big(\frac{d-1}{2}\big)N_e \ . \tag{2.36}$$

[15] Charge conjugation is a symmetry of QED.
[16] The electromagnetic current operator j^μ is defined as $j^\mu \equiv \bar{\psi}\gamma^\mu\psi$

From this equation, we see that the independence of the number of vertices is not universal. For high-enough dimensional QED, i.e. $d > 4$, *all* amplitudes are divergent if one considers higher orders in perturbation theory. Such theories are called *non-renormalizable*. If we consider $d < 4$, we see from equation 2.36 that diagrams with more vertices have a lower degree of divergence so there are only a finite number of divergent diagrams. Such a theory is called a *super-renormalizable theory*.

The identifications can also be made by looking at the (mass-)dimension of the coupling constant. In a super-renormalizable theory, the coupling has a positive mass dimension. If the coupling is dimensionless, the theory is renormalizable, whereas a negative mass dimension indicates a non-renormalizable theory.

2.3.2 Cutoff regularization

The term regularization refers to the procedure that is used to modify a (divergent) integral to make it dependent on some parameter. The divergent behaviour of the integral is then 'encoded' in the parameter. The ultraviolet (UV) infinities originate from the fact that we allow the momenta of our virtual particles to become arbitrarily high. This corresponds to the assumption that our field theory is valid to arbitrarily small length scales. This naturally suggests a way to handle the infinities: cut off the divergent integral at a large momentum Λ. The value of the cutoff is often set to a scale at which the theory is known to break down. For the SM this is the Planck scale $M_{Pl} \approx 1,2 \cdot 10^{19}$ GeV, where the effects of gravity can no longer be neglected. This means that, using the cutoff method we replace:

$$\int_0^\infty dl_E^2 \to \int_0^{\Lambda^2} dl_E^2 \ , \tag{2.37}$$

where we've considered an integral that has already been Wick-rotated, such that the Minkowskian integral is turned into a Euclidean one. The integration variable is changed to $l_e^2 = (L_E^0)^2 + (L_E^1)^2 + (L_E^2)^2 + (L_E^3)^2$. By using this method of regularization, we only look at length scales $L \gtrsim 1/\Lambda$. This method of regularization breaks translational invariance in momentum space and can be somewhat awkward to work with, despite its intuitive nature.

Here, we show an example of a calculation using cutoff regularization, during which we shall carelessly ignore all prefactors. Consider the following integral:

$$\int d^4p \frac{1}{p^2 - m^2} \xrightarrow{\text{Wick}} \int d\Omega_3 \int_0^\infty dp_E \frac{p_E^3}{p_E^2 + m^2} \ . \tag{2.38}$$

The first integral is over the angles of the three-sphere. The divergent part is contained in the second integral over the absolute value of the Euclidean momentum. Next, the cutoff method is applied to the second integral:

$$\int_0^\Lambda dp_E \frac{p_E^3}{p_E^2 + m^2} = \frac{1}{2}\Big[p_E^2 - m^2 \log\left(p_E^2 + m^2\right)\Big]_0^\Lambda = \frac{\Lambda^2}{2} + \frac{m^2}{2} \log\left(\frac{m^2}{\Lambda^2 + m^2}\right) \ . \tag{2.39}$$

The final answer obviously depends on the value of the cutoff. The leading term in the limit $\Lambda \to \infty$ is the quadratic term. We see that this integral is indeed quadratically divergent, as was to be expected from naive powercounting.

2.3.3 Dimensional regularization

As stated in section 2.3.2, regularization using the cutoff method has some downsides, mainly the breaking of translational invariance. This in term causes the Ward identity to be violated in some cases. Instead of working with these challenges, a different regularization scheme, called *dimensional regularization* (DREG)[14], is often used. In this regularization scheme, field modes of arbitrarily high momenta remain, but the calculations are performed in a non-integer number of dimensions by taking an analytic continuation of the number of spacetime dimensions[17] to $d = 4 - \epsilon$. Only at the end of our calculation (after renormalization) we take the limit $\epsilon \downarrow 0$. Changing the number of dimensions changes the mass dimension of the integral. So to keep the right units, we introduce an arbitrary energy scale μ_D^{4-d}. For an arbitrary Feynman integral, where the numerators have been combined using Feynman parameters[18], the process of dimensional regularization is as follows:

$$\int \frac{d^4 l}{(2\pi)^4} \frac{1}{(l^2 - \Delta)^n} \to \mu_D^{4-d} \int \frac{d^d l}{(2\pi)^d} \frac{1}{(l^2 - \Delta)^n} \xrightarrow{\text{Wick}} \mu_D^{4-d} \int \frac{d^d l_E}{(2\pi)^d} \frac{i(-1)^n}{(l_E^2 + \Delta)^n} \ . \tag{2.40}$$

In the first step, we've introduced DREG and in the second step the integral was Wick rotated to provide us with d equivalent dimensions.[19] The right-hand side can then be written as:

$$\mu_D^{4-d} i(-1)^n \int \frac{d\Omega_d}{(2\pi)^d} \int_0^\infty d|\vec{l_E}| \frac{l_E^{d-1}}{(l_E^2 + \Delta)^n} \ . \tag{2.41}$$

The first of these integrals is simply the surface area of a d-dimensional sphere, which is given by:

$$\int d\Omega_d = \frac{2\pi^{d/2}}{\Gamma(d/2)} \ , \tag{2.42}$$

where $\Gamma(x)$ is the Gamma function, which has the useful property that $\Gamma(n+1) = n\Gamma(n)$.
The second integral can also be evaluated, it does require some handy substitutions which we shall not reproduce here. The results of both integrals combined allows us to calculate our Feynman integral:

$$\mu_D^{4-d} \int \frac{d^d l}{(2\pi)^d} \frac{1}{(l^2 - \Delta)^n} = \mu_D^{4-d} \frac{(-1)^n i}{(4\pi)^{d/2}} \frac{\Gamma(n - \frac{d}{2})}{\Gamma(n)} \Big(\frac{1}{\Delta}\Big)^{n - \frac{d}{2}} \ . \tag{2.43}$$

The same methods can be applied to other common loop integrals to find the results of appendix B.1.
Now, if the integral converges, one could easily set d equal to 4. If the integral diverges, as is often the case, one can extract the behaviour near $d = 4$ by expanding with respect to ϵ. Doing this for $n = 2$ results in:

$$\mu_D^{4-d} = \mu_D^{\epsilon} = 1 + \epsilon \log(\mu_D) + \mathcal{O}(\epsilon^2) \ , \tag{2.44}$$

$$\Big(\frac{1}{\Delta}\Big)^{2 - \frac{d}{2}} = \Delta^{-\frac{\epsilon}{2}} = 1 - \frac{\epsilon}{2} \log(\Delta) + \mathcal{O}(\epsilon^2) \ , \tag{2.45}$$

$$(4\pi)^{-d/2} = (4\pi)^{\frac{\epsilon}{2} - 2} = (4\pi)^{-2}\big(1 + \frac{\epsilon}{2}\log(4\pi) + \mathcal{O}(\epsilon^2)\big) \ , \tag{2.46}$$

$$\Gamma(2 - \frac{d}{2}) = \Gamma\big(\frac{\epsilon}{2}\big) = \frac{2}{\epsilon} - \gamma_E + \mathcal{O}(\epsilon) \ . \tag{2.47}$$

Applying these approximations to the integral of equation 2.43 for $n = 2$ results in:[20]

$$\mu_D^{4-d} \int \frac{d^d l}{(2\pi)^d} \frac{1}{(l^2 - \Delta)^2} = \frac{i}{(4\pi)^2}\Big(\frac{2}{\epsilon} - \gamma_E - \log\big(\frac{\Delta}{\mu_D^2}\big) + \log(4\pi)\Big) + \mathcal{O}(\epsilon) \ . \tag{2.48}$$

[17] In the literature, sometimes the convention $d = 4 - 2\epsilon$ is used for reasons that will become clear later.
[18] We'll explicitly use Feynman paramaters later in this work. For an overview of how this mathematical trick works, see appendix D.1.
[19] Note that, in DREG the actual number of dimensions changes from 1+3 to $1 + (3 - \epsilon)$. This allows us to perform Wick rotation as usual.
[20] If the convention of $d = 4 - 2\epsilon$ was chosen, the $2/\epsilon$ would be $1/\epsilon$, and there would be no square inside the logarithm.

We notice that the diverging behaviour is now encoded in the $\frac{1}{\epsilon}$-term. DREG has allowed us to work out the integral, resulting in a convergent answer as long as one does not consider the limit $\epsilon \downarrow 0$.
We've seen that DREG works very well for logarithmically divergent integrals. The small dimensional deviation renders the integrals convergent. Later in this work DREG will be used for quadratic divergencies as well. One can wonder if the change in number of dimensions is still warranted. Applying DREG to quadratically divergent integrals results in the same $\frac{1}{\epsilon}$-term. It is sometimes stated that DREG is 'blind' to the type of divergence. We will come back to these possible issues in great detail later in section 4.

2.4 Renormalization

In this section the idea of renormalization is discussed. This section will begin with the introduction of counterterms in the Lagrangian. In the second part, two (relevant) renormalization schemes will be explained: MS (or $\overline{MS}$) and OS. After this, the running of parameters will be discussed, leading to the Renormalization Group Equation (RGE).
In the previous section, the infinite part of the loop integral has been 'put into a parameter'. Now it is necessary to 'get rid' of this parameter. The answer of a calculation cannot depend on some arbitrarily chosen parameter like Λ or ϵ. The process of re-expressing observables in terms of observables[21] is called *renormalization*. It is often stated that renormalization is needed because of the infinities that come up in loop calculations. This is not completely true: the renormalization procedure is necessary because perturbation theory is used and would still be needed if *all* calculations would yield finite results [15]. This is often called finite renormalization.

2.4.1 Counterterms

The first step in the renormalization procedure, is to realize that the (values of the) parameters in the Lagrangian are not the same as the values measured in experiments. We can make use of this to rewrite the Lagrangian in terms of physically measurable parameters. The 'old' parameters in the Lagrangian are labelled with an index-0 (e.g. m_0) and are called the *bare parameters*.
We'll start by rescaling the fields that appear in the Lagrangian to absorb field-strength renormalizations; effectively we write "Field" $= Z_i^{1/2}$"Field"$_r$, where the index r indicates the rescaled field. We'll use Z_2 for Dirac fields and Z_3 for photon fields. This step ensures that the expressions for the propagators have the form as mentioned in the Feynman rules in appendix C. This step introduces factors of Z_i in the Lagrangian. After this first step, the QED Lagrangian for an electron becomes:

$$\mathcal{L} = -\frac{1}{4} Z_3 (F_r^{\mu\nu})^2 + Z_2 \bar{\psi}_r (i\partial\!\!\!/ - m_0)\psi_r - e_0 Z_2 Z_3^{1/2} \bar{\psi}_r \gamma^\mu \psi_r A_{r\mu} \ , \tag{2.49}$$

where the indices for the field-strength renormalizations follow the convention from [7].
Next, we split each term in the Lagrangian, where we indicate the physical mass[22] of the electron by m and the physical strength of the electromagnetic coupling by $e = -|e|$, i.e. the observable charge of the electron. The Lagrangian then becomes:

$$\begin{aligned} \mathcal{L} = &-\frac{1}{4}(F_r^{\mu\nu})^2 + \bar{\psi}_r (i\partial\!\!\!/ - m)\psi_r - e\bar{\psi}_r \gamma^\mu \psi_r A_{r\mu} \\ &- \frac{1}{4}\delta_3 (F_r^{\mu\nu})^2 + \bar{\psi}_r (i\delta_2 \partial\!\!\!/ - \delta_m)\psi_r - e\delta_1 \bar{\psi}_r \gamma^\mu \psi_r A_{r\mu} \ , \end{aligned} \tag{2.50}$$

[21] Or observables in terms of measured quantities.
[22] So m is the location of the pole in the propagator.

with:[23]

$$\delta_3 = Z_3 - 1, \quad \delta_2 = Z_2 - 1, \quad \delta_m = Z_2 m_0 - m \quad \text{and} \quad \delta_1 = Z_1 - 1\ . \tag{2.51}$$

We now notice two things. First of all, the first line of equation 2.51 is simply our original Lagrangian, but with all Lagrangian parameters and fields replaced by physical observables and rescaled fields respectively. The second line introduces new terms and is called the *Counterterm Lagrangian*. The extra terms in the Lagrangian also introduce new Feynman rules which have to be taken into account when calculating amplitudes. The new Feynman rules are also summarized in appendix C. Note that it is often stated that counterterms are *added* to a Lagrangian, however in the procedure described above, we've not added anything, the Lagrangian has simply been rewritten. The rescaling of the fields has been made explicit here to illustrate what's happening. In the rest of this work we'll omit the index r on the rescaled fields.

2.4.2 (Modified) Minimal Subtraction

At this point, one can define the counterterms in such a way that, when calculating amplitudes, the counterterm diagrams cancel the divergent parts introduced by the 'normal' diagrams. In this minimal *renormalization scheme* there are no conditions imposed on the amplitudes. In simple terms, what is done is simply subtracting the pole at $\epsilon = 0$. This scheme is called *Minimal Subtraction* (MS).
A similar scheme that is often used is the *Modified Minimal Subtraction*-scheme, denoted by $\overline{MS}$ [24]. In this scheme, not only the divergent part is cancelled by the counterterms, but also the constants γ_E and $\log(4\pi)$ that appear in loop calculations using DREG.

2.4.3 OS-Scheme

Another renormalization scheme is called the on-shell (OS) scheme. Here, we specify renormalization conditions which define the physical couplings and masses. Each of the counterterms has to be specified by a renormalization condition. Before stating the conditions for QED, let us introduce some notation for (sets of) QED diagrams. We'll indicate the momentum carried by photon propagators by q and the momentum carried by fermionic propagators by p.

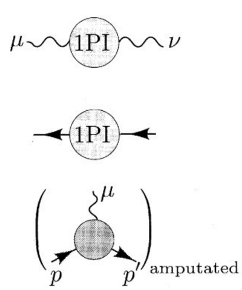

$$= i\Pi^{\mu\nu}(q) = i(g^{\mu\nu}q^2 - q^\mu q^\nu)\Pi(q^2),$$

$$= -i\Sigma(\not{p}),$$

$$= -ie\Gamma^\mu(p', p).$$

Figure 5: Notation for different QED amplitudes for electrons [7].

In the last set 'amputated' means that the external lines are removed, but the momenta flowing through them is kept and p and p' are the fermionic momenta. The next step in the procedure is to calculate these

[23] The scaling factor Z_1 helps to 'fix' the definition of the electric charge and is defined by $e_0 Z_2 Z_3^{1/2} \equiv e Z_1$.
[24] $\overline{MS}$ is pronounced 'em-ess-bar'.

amplitudes and define the physical parameters and keep the field-strength renormalizations equal to 1 (i.e. the residues of the propagators). Explicitly, the four conditions are:

$$\begin{aligned}
\hat{\Sigma}(\not p = m) &= 0; \\
\frac{d}{d\not p}\hat{\Sigma}(\not p)\big|_{\not p = m} &= 0; \\
\hat{\Pi}(q^2 = 0) &= 0; \\
-ie\hat{\Gamma}^{\mu}(p' - p = 0) &= -ie\gamma^{\mu} \ .
\end{aligned} \tag{2.52}$$

Here, a specific momentum scale has been chosen to fix the values of the parameters. The first condition fixes the electron mass at m, whereas the next two conditions fix the residues of the propagators at 1. The last condition fixes the charge of the electron to be e. The 'hats' indicate that we're dealing with renormalized quantities, i.e. including counterterms.

2.4.4 Renormalized QED at one loop

Next, the counterterms (at one-loop level) will be calculated explicitly to satisfy the renormalization conditions introduced in equation 2.52. This section will also introduce some of the tools encountered in performing loop calculations.

Electron self-energy

Let us begin with a careful examination of the electron self-energy. The unrenormalized self-energy (at one loop) is given by:

$$-i\Sigma_e^{(1)}(\not p) = \tag{2.53}$$

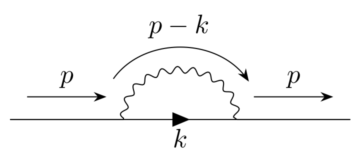

The diagram is given by:

$$\int \frac{d^4k}{(2\pi)^4}(-ie\gamma^{\mu})\Big(\frac{i}{\not k - m}\Big)\Big(\frac{-ig_{\mu\nu}}{(p-k)^2}\Big)\big(-ie\gamma^{\nu}\big) \ . \tag{2.54}$$

From this we already notice that the integral has an infrared (IR) divergence, which can be regularized by adding a small photon mass, as is done in [7]. Within this thesis the focus is on ultraviolet (UV) divergencies, so we will not bother (too much)[25] with the infrared divergence that occurs here. However it can be shown that the IR divergencies encountered in the virtual photons cancel against IR divergencies introduced by real photon emission in the calculation of amplitudes [16]. Furthermore, the integral has a UV divergence, which we will regularize using DREG. We then find:

$$-i\Sigma_e^{(1)}(\not p) = -e^2\mu_D^{\epsilon}\int \frac{d^dk}{(2\pi)^d}\Big(\frac{\gamma^{\mu}\gamma^{\nu}\gamma_{\mu}k_{\nu}}{(k^2-m^2)[(p-k)^2 - m_{\gamma}^2]} + \frac{\gamma^{\mu}m\gamma_{\mu}}{(k^2-m^2)[(p-k)^2-m_{\gamma}^2]}\Big) \ . \tag{2.55}$$

Next, we'll rewrite the denominators using Feynman parameters (see appendix D.1):

$$\frac{1}{(k^2-m^2)[(p-k)^2-m_{\gamma}^2]} = \int_0^1 dx[k^2 - 2xk\cdot p + xp^2 - xm_{\gamma}^2 - (1-x)m^2]^{-2} \ , \tag{2.56}$$

[25] We'll simply add a small mass for the photon (m_{γ}) and not worry about it.

after which we'll shift the integration variable $l \equiv k - xp$ to find:

$$\int d^d k \frac{1}{(k^2 - m^2)[(p-k)^2 - m_\gamma^2]} = \int_0^1 dx \int d^d l \frac{1}{[l^2 - \Delta]^2} \; , \tag{2.57}$$

with $\Delta \equiv -x(1-x)p^2 + xm_\gamma^2 + (1-x)m^2$.
The next step is to write out the contractions of the gamma matrices. Notice that in $d = 4 - \epsilon$ dimensions we have (see appendix D.2):

$$\gamma^\mu \gamma^\nu \gamma_\mu = -(2-\epsilon)\gamma^\nu, \quad \gamma^\mu \gamma_\mu = d \; . \tag{2.58}$$

So for the self-energy, the expression becomes:

$$-i\Sigma_e^{(1)}(\not{p}) = -e^2 \mu_D^\epsilon \int_0^1 dx \int \frac{d^d l}{(2\pi)^d} \Big(\frac{-(2-\epsilon)(\not{l} + x\not{p})}{[l^2 - \Delta]^2} + \frac{(4-\epsilon)m}{[l^2 - \Delta]^2} \Big) \; . \tag{2.59}$$

The integral that is linear in l in the numerator is odd under $l \to -l$ and will evaluate to 0. Using expression 2.43 we find:

$$-i\Sigma_e^{(1)}(\not{p}) = -i \frac{e^2 \mu_D^\epsilon}{(4\pi)^{d/2}} \int_0^1 dx \frac{\Gamma(2 - \frac{d}{2})}{\Delta^{2-d/2}} \Big((4-\epsilon)m - (2-\epsilon)x\not{p} \Big) \; , \tag{2.60}$$

where it might be tempting to take the limit of $\epsilon \to 0$, but we have to realize that there is an ϵ-pole in the expansion of the gamma function. We are now in a position to perform the renormalization procedure. This is done by adding the counterterm-diagram to the expression of the self-energy, so that:

$-i\hat{\Sigma}_e^{(1)}(\not{p}) =$ 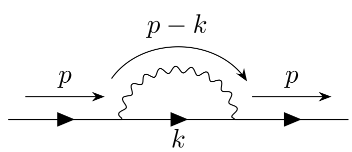 $+$ 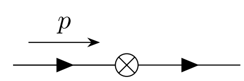 , (2.61)

where the 'hat' was added to Σ to indicate that the self-energy is now renormalized. The counterterm diagram simply evaluates to $i(\not{p}\delta_2 - \delta_m)$, where δ_2 and δ_m are fixed by the renormalization conditions from equation 2.52. The first of these conditions tells us:

$$m\delta_2 - \delta_m = \frac{e^2 m \mu_D^\epsilon}{(4\pi)^{d/2}} \int_0^1 dx \frac{\Gamma(2 - \frac{d}{2})(4 - 2x - \epsilon(1-x))}{[(1-x)^2 m^2 + xm_\gamma^2]^{2-d/2}} \; . \tag{2.62}$$

Expressions like these can be approximated using equations 2.44-2.47, which shall not be done at this point. Note, however, that the terms proportional to ϵ do give a finite result in the limit $\epsilon \to 0$, as it is multiplied by the ϵ-pole in the divergent gamma function.
For the second condition, the derivative of the self-energy with respect to $\not{p}$ is needed. Because the self-energy depends on both $\not{p}$ and p^2, implicit differentiation is used:

$$\frac{d}{d\not{p}} = \frac{\partial}{\partial \not{p}} + \frac{dp^2}{d\not{p}} \frac{\partial}{\partial p^2} = \frac{\partial}{\partial \not{p}} + 2\not{p} \frac{\partial}{\partial p^2} \; . \tag{2.63}$$

This allows us to find:

$$\delta_2 = \frac{d}{d\not{p}} \Sigma_e^{(1)}(\not{p}) \big|_{\not{p}=m} = -\frac{e^2 \mu_D^\epsilon}{(4\pi)^{d/2}} \int_0^1 dx \frac{\Gamma(2 - d/2)}{((1-x)^2 m^2 + xm_\gamma^2)^{\epsilon/2}} \times \\ \Big((2-\epsilon)x - \epsilon \frac{x(1-x)m^2}{(1-x)^2 m^2 + xm_\gamma^2} (4 - 2x - \epsilon(1-x)) \Big) \; . \tag{2.64}$$

At this point, it is not the exact form of these expressions that is of interest to us, it is the method that is used to calculate the counterterms, such that the renormalized mass parameter actually corresponds to the physical mass of the particle. With a careful examination of the expressions given above, the cancellation of divergent terms can be seen explicitly. We will see this cancellation explicitly in the scalar model that will be introduced in section 4.

Photon self-energy
In the same manner as done with the electron self-energy, we can investigate the photon self-energy at momentum q, which is given by:

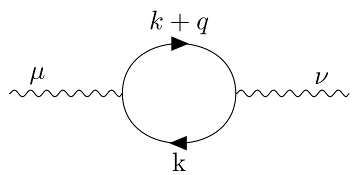

Figure 6: Photon self-energy diagram.

Following the Feynman rules, this diagram results in:

$$(-ie)^2(-1)\int \frac{d^4k}{(2\pi)^4}\,\text{Tr}\left[\gamma^\mu \frac{i}{\not{k}-m}\gamma^\nu \frac{i}{\not{k}+\not{q}-m}\right] \equiv i\Pi^{\mu\nu}(q)\ , \tag{2.65}$$

where the factor of (-1) comes from the fermion loop. Before calculating the trace, applying DREG and performing the loop integral, let us 'guess' the form of the answer. The only objects that can carry the Lorentz structure required are the metric tensor $g^{\mu\nu}$ and the (only available) momentum tensor $q^\mu q^\nu$. However, we know from the Ward identity that $q_\mu \Pi^{\mu\nu} = q_\nu \Pi^{\mu\nu} = 0$. This implies that the photon self-energy is proportional to the projection operator $(g^{\mu\nu} - q^\mu q^\nu / q^2)$. Factoring out this tensor structure, we find:

$$\Pi^{\mu\nu}(q) = (q^2 g^{\mu\nu} - q^\mu q^\nu)\Pi(q^2). \tag{2.66}$$

The arguments of section 2.2.3 can be repeated to find a general expression for the photon self energy (at any loop level)[7]:

$$\frac{-g_{\mu\nu}}{q^2(1-\Pi(q^2))}\ , \tag{2.67}$$

which has a pole at $q^2 = 0$. Hence the Ward Identity makes sure that the photon stays massless at all orders in perturbation theory.
The full calculation of the photon self-energy of diagram 6 can be found in appendix E.1, the result is:

$$i\Pi^{\mu\nu}(q) = (q^2 g^{\mu\nu} - q^\mu q^\nu)\cdot \frac{-8ie^2\mu_D^\epsilon}{(4\pi)^{d/2}}\int_0^1 dx\ x(1-x)\frac{\Gamma(2-d/2)}{\Delta^{2-d/2}}\ , \tag{2.68}$$

where $\Delta \equiv m^2 - x(1-x)q^2$.

We can now add the counterterm diagram,

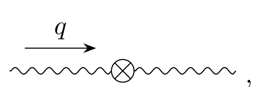

Figure 7: Counterterm diagram contribution to the photon self-energy.

to the expression of the self energy and impose the renormalization condition $\hat{\Pi}(q^2 = 0) = 0$ to find:

$$\delta_3 = \Pi(0) = -\frac{8e^2\mu_D^\epsilon}{(4\pi)^{d/2}} \int_0^1 dx\; x(1-x)\frac{\Gamma(2-d/2)}{(m^2)^{2-d/2}}\;. \tag{2.69}$$

2.5 Running of couplings and scheme dependence

In the last section, the OS-scheme was used to set up a renormalized version of QED. During the regularization procedure, the scale μ_D was introduced, but in the final version of the renormalized theory, this scale does not show up. This is not surprising; the OS-renormalization scheme is set up to perform subtractions at a fixed scale and anchor observables by performing a measurement. In the OS-scheme the scale at which the parameters are fixed is at the scale where the momentum is equal to the mass of the particle (hence the name 'on-shell'). Due to the renormalization conditions, the dependence on μ_D drops out.
In the MS/$\overline{MS}$-scheme this is not the case and μ_D still appears in the expressions after renormalization. Because the energy scale at which the renormalization is performed is arbitrary, the final answer of the calculation of a matrix element cannot depend on it, hence we impose:

$$\mu_D \frac{d\mathcal{M}}{d\mu_D} = 0 \tag{2.70}$$

Because our matrix element (calculated using MS/$\overline{MS}$) has an explicit dependence on μ_D, the only way equation 2.70 can hold, is if the parameters also depend on μ_D, so we can rewrite:

$$\Big[\mu_D \frac{\partial}{\partial\mu_D} + \mu_D\frac{d\lambda}{d\mu_D}\frac{\partial}{\partial\lambda} + \mu_D\frac{dm}{d\mu_D}\frac{\partial}{\partial m}\Big]\mathcal{M} = 0 \tag{2.71}$$

From these equations, some *renormalization group equations* (RGE's) can be determined, which determine the dependence of the parameters on the energy scale. For example, the so-called β-function captures the dependence of the coupling via:

$$\beta(\lambda) = \mu_D\frac{d\lambda}{d\mu_D} = \frac{d\lambda}{d(\log(\mu_D)} \tag{2.72}$$

This equation describes the 'running of the coupling' with energy scales. In QED the coupling is the charge, but the running parameter is often stated in terms of α, which at low energies is $\alpha \approx 1/137$. At higher energies, the value of α changes, for example at an energy of 100 GeV we find $\alpha \approx 1/128$.

Equation 2.71 ensures that, if we take into account *all* orders, the chosen reference scale μ_D does not matter. However, if one chooses the reference scale in a smart manner, there are fewer orders in perturbation theory needed to find an accurate answer. When doing calculations, the scale that is chosen often is of the order of the energy scales of the particles involved. The 'smart' choice ensures that the logarithms, in which μ_D appears, are suppressed.

2.6 Fine-tuning

In section 2.2.3 we've seen that the observable mass of a particle comes from two parts. Firstly there is the bare parameter in the Lagrangian and secondly there are the quantum corrections in the form of self-energy diagrams. For the Higgs boson, the mass would be given by:

$$m_h^2 = m_0^2 + \delta_{m_h}^2\;, \tag{2.73}$$

were the bare mass m_0 is indicated with the index 0 and the corrections are captured in the $\delta_{m_h}^2$ term. This relation is not new to the Higgs boson; all particles receive quantum corrections to their masses. Furthermore,

if the corrections are of the order of the bare mass ($\delta^2_{m_h} \lesssim m_0^2$) there are no problems. For all the particles in the SM that have to be included in the Higgs self-energy diagrams, there are no problems. However, we cannot be sure that there are no particles beyond the SM. If there is beyond the standard model (BSM) physics, these (undiscovered) particles would give further corrections to the Higgs mass. As we'll see later (and can be seen in [6]), a fermion adds a contribution to $\delta^2_{m_h}$ of the order of m_f^2. This result holds when the calculations are done using MS or $\overline{MS}$. It was observed by Reijns [6] that (at least at one-loop order) the corrections are of $\mathcal{O}(1)$ when using OS renormalization. In the literature, the problem of fine-tuning arises when one considers BSM physics. Let the scale where new particles enter the picture be $\simeq \Lambda$. Then the argument is that these particles cause $\mathcal{O}(\Lambda^2)$ shifts in the Higgs mass. To still find the (relatively) low Higgs mass that we observe, we need to tune the bare parameter m_0 to very high accuracy to cancel the entire contribution from the heavy particle *except* for 125 GeV. In a sense, we need to fine-tune the parameters to get the values that are observed in experiment. For this reason, this is called the fine-tuning problem.
Note that other particles in the SM also undergo quantum corrections to their masses. However, gauge bosons are 'protected' by symmetries (like the Ward Identity). The fermions in the SM are protected by a chiral symmetry. The Higgs boson does not posses such a symmetry to protect it from these corrections. Throughout the years there have been numerous solutions to this problem. One of which is the idea of supersymmetry, where an extra symmetry is added to the system to provide 'protection' to the Higgs boson. In a supersymmetric theory, every particle has a supersymmetric partner-particle. The supersymmetric partners of fermions are bosons and vice-versa. This causes a natural cancellation between the corrections (as the contributions by fermions automatically introduce a minus sign).
Another solution is the idea of *composite Higgs* models. In these models the Higgs boson is not treated as an elementary particle but it is a bound state of new interactions. The corrections to the mass of the composite Higgs particle are then automatically cut off by the compositeness scale (Λ_C).

3 Appelquist-Carazzone Decoupling Theorem

The main focus of this work is on (renormalizable) theories that include different mass scales. The influence of the heavy fields on the low-energy behaviour of the theory will be investigated. In this section, the work of Appelquist and Carazzone will be reproduced. By investigating the proof we'll understand how and why heavy fields effectively decouple in processes with no external heavy particles. The relevance of the decoupling of heavy fields is that the low-energy behaviour of the theory can then be described by an Effective Field Theory (EFT) where the heavy fields have been integrated out. The EFT is described by a renormalizable Lagrangian containing only the light fields.

Before we go into the proof of the decoupling theorem, let us explore a well known example. In section 2.4.4 we've calculated the photon self-energy at one loop. The result of this calculation (including the counterterm) is given by:

$$\begin{aligned} i\hat{\Pi}^{\mu\nu}(q) = (q^2 g^{\mu\nu} - q^\mu q^\nu)\Big[&\frac{-8ie^2\mu_D^\epsilon}{(4\pi)^{d/2}}\int_0^1 dx\ x(1-x)\frac{\Gamma(2-d/2)}{\Delta^{2-d/2}} \\ &+ \frac{8ie^2\mu_D^\epsilon}{(4\pi)^{d/2}}\int_0^1 dx\ x(1-x)\frac{\Gamma(2-d/2)}{(m^2)^{2-d/2}}\Big]\ , \end{aligned} \tag{3.1}$$

where $\Delta \equiv m^2 - x(1-x)q^2$.

We'll investigate this self energy in the limit of a very heavy fermion (or similarly a low energy limit for the photon). In that case the energy of the photon is nowhere near high enough to produce on shell fermions. Let us see if the quantum correction by the heavy virtual particles running around in a loop has any observable effect. We'll start by using the approximations from equations 2.44-2.47 to rewrite the renormalized self energy. Because this is the first time in this work that we apply these approximations, we'll write them out completely:

$$\begin{aligned} i\hat{\Pi}^{\mu\nu}(q) &= (q^2 g^{\mu\nu} - q^\mu q^\nu)8ie^2\int_0^1 dx\ x(1-x)\Big[\big(1+\epsilon\log(\mu_D)+\mathcal{O}(\epsilon^2)\big)(4\pi)^{-2}\big(1+\frac{\epsilon}{2}\log(4\pi)+\mathcal{O}(\epsilon^2)\big) \\ &\qquad \big(\frac{2}{\epsilon}-\gamma_E+\mathcal{O}(\epsilon)\big)\big(1-\frac{\epsilon}{2}\log\big(m^2\big)-1+\frac{\epsilon}{2}\log(\Delta)+\mathcal{O}(\epsilon^2)\big)\Big] \\ &= (q^2 g^{\mu\nu} - q^\mu q^\nu)\frac{8ie^2}{(4\pi)^2}\int_0^1 dx\ x(1-x)\Big[\log\Big(\frac{\Delta}{m^2}\Big)+\mathcal{O}(\epsilon)\Big]\ . \end{aligned} \tag{3.2}$$

In the context of the decoupling theorem, we're interested in the low-energy behaviour of the self energy and we can use the fact that $q^2 \ll m^2$ to expand the logarithm in equation 3.2, resulting in[26,27]:

$$i\hat{\Pi}^{\mu\nu}(q) = (q^2 g^{\mu\nu} - q^\mu q^\nu)\frac{8ie^2}{(4\pi)^2}\int_0^1 dx\ x(1-x)\Big[-x(1-x)\frac{q^2}{m^2}+\mathcal{O}\big(\frac{q^4}{m^4},\epsilon\big)\Big]\ . \tag{3.3}$$

From this expression for the photon self-energy we see that, after renormalization (which has taken care of the logarithmic divergence) the only effect of the heavy particle scales proportional to an inverse power of m; the heavy fields effectively decouple when studying the low-energy behaviour of the theory.

The next section will prove the decoupling of a heavy field from low-energy physics in a much more general theory.

[26]It was also used that $0 \leq x \leq 1$.

[27]We'll use the notation $\mathcal{O}(a, b)$ to denote higher order terms in a and b to keep the notation from getting too cluttered.

3.1 Setting the scene

Even though the Appelquist-Carazzone decoupling theorem is quite general, the proof that we'll provide will be for a specific model. This model consists of massless gauge fields $A_{\alpha\mu}(x)$ and heavy spin-$\frac{1}{2}$ fields $\psi_n(x)$. The Lagrangian for this theory is given by[28]:

$$\mathcal{L}(x) = -\frac{1}{4} F^a_{\mu\nu} F_a^{\mu\nu} - \bar{\psi} \not{D} \psi - \bar{\psi} m \psi - \delta m \bar{\psi} \psi \ , \tag{3.4}$$

with

$$F^a_{\mu\nu} \equiv \partial_\mu A^a_\nu - \partial_\nu A^a_\mu + g f^{abc} A_{b,\mu} A_{c,\nu} \ . \tag{3.5}$$

The covariant derivative is defined by:

$$(D_\mu \Psi)_n = \partial_\mu \Psi_n - i g A^a_\mu [T^a \psi]_n \ , \tag{3.6}$$

with the Lie algebra of the gauge group defined by $[T_a, T_b] = i f_{abc} T^c$. The coupling is indicated by g and δm is the mass counterterm, which is adjusted to make the 1PI fermion self energy vanish at $\not{p} = m$ to each order in perturbation theory. The decoupling theorem states [17]:

Consider any 1PI Feynman diagram with external bosons only, but containing internal fermions. When all external momenta are small relative to m^2, then apart from coupling constant and field strength renormalization the diagram will be suppressed by some power of m relative to a diagram with the same number of external bosons but no internal fermions.

Consider the low momentum behaviour of the theory. The decoupling theorem will be proven by considering different cases. First we'll consider the case where the diagram under consideration is UV convergent, meaning that the diagram and *all* of its subdiagrams are superficially convergent. Afterwards we'll consider the case where there are UV divergences.

3.2 Degree of divergence

Before we consider these cases, let us investigate the degree of divergence for our diagrams. We're investigating 1PI diagrams with only external bosons. Note that the restriction on 1PI diagrams circumvents the possible difficulties encountered in section 2.3.1. We will first establish the fact that the degree of divergence of such a Feynman diagram with N_b external bosons is $D = 4 - N_b$. To see this, we'll introduce the following notation:

N_b: The number of external bosons;

N_f: The number of external fermions (which is 0);

P_b: The number of boson propagators;

P_f: The number of fermion propagators;

L: The number of loops in the diagram.

There are three possible interaction vertices in this theory, which will be indicated by:

[28] The notation is slightly different compared to [17] to be more in line with the rest of this thesis.

V: The gauge interaction with two fermions[29] and a gauge boson;

V_3: Triple Gauge Coupling (TGC);

V_4: Quartic Gauge Coupling (QGC).

We'll repeat the reasoning of section 2.3.1 to find the degree of divergence:

$$D = 4L + V_3 - P_f - 2P_b \; . \tag{3.7}$$

This formula follows from powercounting; each loop adds an (four dimensional) integral over the undetermined momentum, each fermion propagator 'removes' one power of momentum and each boson propagator removes two powers of momenta. Note that the TGC also adds one power of momentum.[30] We'd like to express the degree of divergence in terms of external particles, so that the expression does not have to depend on the inner workings of the diagram. To this end, we look at the amount of vertices in the diagram which is given by:

$$\begin{aligned} &4V_4 + 3V_3 + V = N_b + 2P_b \; ; \\ &2V = 2P_f \rightarrow V = P_f \; . \end{aligned} \tag{3.8}$$

The second equality holds because the amount of external fermions is zero. From the first equality, it follows that:

$$P_b = 2V_4 + \frac{3}{2}V_3 + \frac{V}{2} - \frac{N_b}{2} \; . \tag{3.9}$$

The amount of loops in a diagram is given by:

$$\begin{aligned} L &= P_f + P_b - V_3 - V_4 - V + 1 \\ &= V_4 + \frac{V_3}{2} + \frac{V}{2} - \frac{N_b}{2} + 1 \; . \end{aligned} \tag{3.10}$$

Inserting these expressions into equation 3.7 we find:

$$\begin{aligned} D = &\, 4V_4 + 2V_3 + 2V - 2N_b + 4 + V_3 - 4V_4 - 3V_3 - V + N_b - V = \\ &= 4 - N_b \; . \end{aligned} \tag{3.11}$$

3.3 The convergent diagrams

The first case we'll examine is the case where the diagram under consideration is UV convergent, so in this case we have $N_b \geq 5$ and there are no divergent subdiagrams. According to the decoupling theorem, diagrams that do contain internal fermions are suppressed relative to diagrams containing no internal fermions. In the scenario without internal fermions, we find that the diagram behaves like k^{4-N_b} where k is the momentum of the external bosons.[31]

Next, consider again a diagram with N_b external bosons, but now containing internal fermions. The fermions always appear in closed loops, because there are no external fermions. We focus on one of these

[29] A fermion and an anti-fermion

[30] This can be seen from the Feynman rule for the TGC, see appendix C.2 equation C.3. It can also be argued by the fact that we have three momenta associated with the vertex, this means that we cannot distribute all Lorentz indices to metric tensors, i.e. one of them has to be carried by a momentum. Note that the QGC does not depend on the momentum, see equation C.4.

[31] Assuming all bosons have momenta of order k.

loops (being a subdiagram of the parent diagram). Attached directly to each fermion loop, there are f 'external' (from the point of view of the subdiagram) boson lines. There are two possibilities; either $f \geq N_b$ or $f < N_B$.
First we'll consider the case where $f \geq N_b$, an example of such an (sub)diagram is:

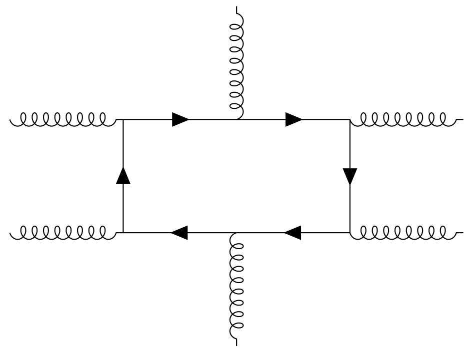

Figure 8: A subdiagram with 6 external bosons.

The degree of divergence of the subdiagram is $D = 4 - f$. Because the fermions in the theory are very heavy and we're considering the low energy limit ($k \ll m$), we can take the limit of $m \to \infty$ in the subdiagram. The subdiagram introduces a loop integral, in which we can shift the loop momentum such that all external momenta can be scaled to zero. The reason that this is possible is that the mass of the fermion is so much higher than the external momenta, so no divergences are encountered. In taking the limit of $m \to \infty$ we've effectively shrunk the subdiagram to a point, so the example diagram of figure 8 becomes:

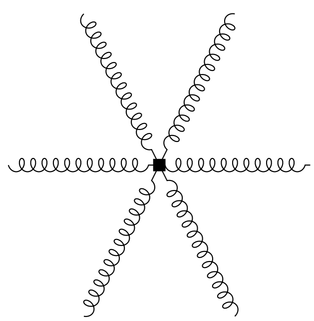

Figure 9: The subdiagram with the fermion loop 'shrunk'.

The subdiagram then behaves like m^{4-f} in the limit of $m \to \infty$. In the bigger parent diagram the shrunken subdiagram behaves like an effective f-point vertex (indicated in figure 3.3 by the square).[32] Here we also see that we only have to look at the 'external' boson lines of the subdiagram; any internal line disappears when the loop shrinks to a point. When we reevaluate the degree of divergence of the parent diagram we need to take into account that the amount of vertices changes:

$$4V_4 + 3V_3 + V + f = N_b + 2P_b \ , \tag{3.12}$$

[32] This effective vertex, at low energies, can be compared to the Fermi coupling in the low energy theory of the weak interactions.

and the number of loops is now given by:

$$L = P_f + P_b - V_3 - V_4 - V - 1 + 1 \; . \tag{3.13}$$

The extra -1 follows from the fact that we now have exactly one extra vertex (the one with f lines). Plugging these equations into equation 3.7 results in a degree of divergence for the reduced diagram 'D_R':

$$D_R = f - N_b \; . \tag{3.14}$$

Interestingly, D_R is the highest degree of divergence to be found anywhere in the diagram. This can be seen from considering different possibilities. Imagine that there are initially two fermion loops both having *at least* 5 boson lines attached. Indicate the amount of boson lines by f and f'. After we've worked through the above process for one of the fermion loops (the one with f bosons, say) the degree of divergence of the overall diagram is $f - N_b \geq 0$, whilst the degree of divergence of the untouched subdiagram (with f' boson legs) is $4 - f' < 0$. This argument easily extends to diagrams with more than two fermion loops.
Because we're considering the case where $f \geq N_b$, the reduced diagram is "divergent" (in the sense of naive power counting), however the argument to find D_R only works for low energies, because when we go to higher and higher loop momenta, the effective vertex in our reduced diagram no longer behaves like a point, so the diagram *looks* divergent, but actually is not.[33] So the reduced diagram behaves like $(\Lambda')^{f-N_b}$, where Λ' indicates the EFT matching scale which is $\mathcal{O}(m)$. The behaviour of the entire diagram is then given by $m^{4-f} m^{f-N_b} = m^{4-N_b}$. This is indeed suppressed compared to k^{4-N_b}. We see that it also does not matter which one of the fermion loops we choose; the dependence on f drops out.
Next, we'll investigate the case where $f < N_b$. Similarly as done above, we investigate the limit of $m \to \infty$ and the fermion loop that has been 'shrunk' behaves like m^{4-f}. This time the degree of divergence of the reduced diagram $D_R = f - N_b < 0$. Now, if there are no other fermion loops, the entire diagram at most behaves like $m^{4-f} k^{f-N_b}$. Here it is important to realize that $f \geq 5$, so that this is indeed suppressed relative to k^{4-N_b}.
If there are even more fermion loops, the argument can be repeated and it is even further suppressed.

3.4 General diagrams

Next, we'll investigate more general diagrams. These diagrams can include divergent (sub)diagrams. We'll start with the case where $N_b = 2$ and $N_b = 3$, as these are the cases where the diagram has the highest degree of divergence.[34] This is comparable to the photon self-energy discussed before. The degree of divergence is given by $D = 4 - N_b$, but is reduced by the transverse structure of the propagator, similar to what was seen with the photon self energy where the Ward identity was invoked to lower the degree of divergence. In the case of a non-Abelian gauge theory, there is the TGC which has a tensor structure carrying three (Minkowski) incices. At least one of these indices has to be carried by an external momentum. This momentum can be factored out, effectively lowering the degree of divergence by one. Combining these two lowers the degree of divergence of diagrams with $N_b = 2$ or $N_b = 3$ to zero. This is not yet convergent, but we still have the counterterm diagrams which 'remove' the logarithmic divergence, effectively lowering the degree of divergence of the combined diagrams to -1. If we have a diagram with $N_b = 4$, the superficial degree of divergence tells us that it is logarithmically divergent so combined with its counterterm diagram we also have a convergent situation. Note that in this section we're actually looking at two behaviours of the diagrams. Above we've

[33] This should come as no surprise, as the act of taking a high mass limit should not make our initially convergent diagram all of a sudden divergent.

[34] The tadpole diagrams (there are now two) automatically vanish due to the same reasoning as in the QED case.

discussed the overall behaviour of a general diagram in terms of the cutoff Λ. The divergence that we've just dealt with is due to the high momenta in the loop and has been reduced by using Ward Identities, the tensor structure of the three-point vertex and by renormalization. Note that the renormalization was performed at a low energy scale $\mu \ll m$,[35] in the example of the photon self-energy this scale was the on-shell mass of the photon (which is 0). In the context of Appelquist-Carazzone, any low-energy renormalization scheme can be used. We will come back to this extensively in the next chapter. Next, we'll look at the behaviour in terms of m. This is similar to what was done at the beginning of this chapter; where we renormalized the photon self-energy after which we investigated how the resulting expression depends on the mass of the heavy particle.

For the general case, we again focus on one of the internal fermion loops. To compare the behaviour later; a diagram without internal fermion lines behaves like k^{4-N_b} (up to logarithms). For the general case, we separate four different cases. To get our definitions clear; when we talk about subdiagrams we explicitly mean the internal fermion loops. The four possibilities are:

1. Divergent parent diagrams with convergent subdiagrams ($f > 4$ and $N_b \leq 4$)
2. Divergent parent diagrams and divergent subdiagrams ($f \leq 4$ and $N_b \leq 4$)
   This splits up in two cases:
   - $f \geq N_b$
   - $f < N_b$
3. Convergent parent diagrams with divergent subdiagrams ($f \leq 4$ and $N_b > 4$)

The first of these cases is similar to the convergent case discussed before. Because the subdiagram is convergent, it shrinks to a point upon taking the limit of $m \to \infty$ and behaves like an extra vertex. The behaviour of the subdiagram is m^{4-f}. The behaviour of the entire diagram is then $k^{f-N_b} m^{4-f} = k^{4-N_b} \left(\frac{k}{m}\right)^{f-4}$ up to logarithms. Because $f > 4$, this is indeed suppressed compared to k^{4-N_b}.

In the second case, the subdiagrams are divergent and we need to take into account the counterterm diagrams. The behaviour of the subdiagram, including the counterterms is:

$$k^{4-f}\left(\log\left(\frac{\Lambda}{m}\right) + \text{constants} + \mathcal{O}\left(\frac{k}{m}\right) - \log\left(\frac{\Lambda}{m}\right) - \text{constants} + \mathcal{O}\left(\frac{\mu}{m}\right)\right) = k^{4-f} \times \text{terms } \mathcal{O}\left(\frac{k}{m}, \frac{\mu}{m}\right) \ . \quad (3.15)$$

The fact that we can factor out the k^{4-f} comes from the tensor structure; in the case of two external bosons the Ward identity is used. In the case of three external bosons, the tensor structure of the TGC is used. Generally, the external bosons carry a Lorentz index which, due to Lorentz covariance, can only be carried by an external momentum or by the metric tensor $g^{\mu\nu}$. After renormalization of the subdiagram, it can again be 'shrunk' to a point. Reevaluating the behaviour of the parent diagram, we find:

$$\underbrace{k^{f-N_b}}_{1} \cdot \underbrace{k^{4-f} \times \text{terms}\mathcal{O}\left(\frac{k}{m}, \frac{\mu}{m}\right)}_{2} = k^{4-N_b} \cdot \mathcal{O}\left(\frac{k}{m}, \frac{\mu}{m}\right) \quad (3.16)$$

where the first factor comes from the 'reduced' parent diagram and the second factor comes from the subdiagram including counterterms. Compared to the diagram without internal fermions, that behaves like k^{4-N_b},

[35] Note that the μ that is used here, refers to the 'subtraction' point of the renormalization. This is not the same parameter as the μ_D that appears in DREG.

this is suppressed.

The next case is similar, but now we have a degree of divergence of the reduced diagram $D_R = f - N_b < 0$. We use the result of the previous case to conclude that the subdiagram behaves like $k^{4-f}\mathcal{O}\left(\frac{k}{m}, \frac{\mu}{m}\right)$, so that (if there are no other fermion loops in the reduced diagram) the reduced diagram behaves like $k^{f-N_b}\mathcal{O}\left(\frac{k}{m}, \frac{\mu}{m}\right)$. If there are fermion loops left in the reduced diagram, the argument can be repeated to induce even further suppression.

The last case can be seen as a special case of the previous case. The treatment of the subdiagram is the same as before and directly causes the suppression compared to the case without internal fermions.

We see that, when there are divergent (sub)diagrams, the method of renormalization becomes important. The degree of divergence of the overall graph is reduced to zero by making use of symmetries, after which renormalization 'removes' the divergent logarithms. Similarly the divergent subdiagrams are renormalized using an arbitrary renormalization point μ. As long as $\mu \ll m$, any point will suffice. Another important point is that the theory under consideration must be renormalizable. An example where the decoupling theorem does not hold, is when considering the weak interactions. If we consider the interactions of hadrons at low energies (a few GeV), the effective theory consists of strong and electromagnetic interactions. This would imply that weak interactions should be ignorable at low energies, however we know that many observed phenomena (e.g. particle decays) are due to the weak interactions. The important thing is that (when weak interactions are absent) the decay of a particle is forbidden (by symmetries such as parity, charge-conjugation and strangeness conservation). Weak interactions at a low energy are described by a non-renormalizable theory (the four-fermion interaction vertex). We cannot assume the decoupling theorem to hold for non-renormalizable theories. Another example that demonstrates that we cannot expect every diagram with internal heavy particles to decouple is the production of Higgs particles through gluon fusion. The calculations for this process are worked out in [6]. The conclusion is that, the diagram *seems* to be suppressed with powers of the heavy mass, but due to the fact that the coupling between the Higgs and fermions depends on the mass of the fermions, the net effect is of order $\mathcal{O}(1)$. Incidentally, this is the reason that we know that there is no (SM-like) fourth generation of fermions. If there was a fourth generation, the Higgs production in particle accelerators would be nine times higher than if this fourth generation was absent. This would definitely be a measurable effect. The reason that this situation does not decouple is due to the fact that the coupling strength scales with the mass of the (heavy) particle and hence introduces the high energy scale to the calculation. Performing subtractions at the low energy scale cannot undo this introduction; the energy scales have been 'mixed'.

3.5 The consequence of $\overline{MS}$, the β-function

In the Appelquist-Carazzone decoupling theorem, the renormalization scheme used is a low-energy renormalization. This can be the OS-scheme but the subtractions can also be performed at an arbitrary off shell Euclidean point (μ), as long as $\mu \ll m$. However, in the literature and in many modern calculations done in QFT, the renormalization scheme used is $\overline{MS}$. Some indications that the use of $\overline{MS}$ can cause 'problems' in (possibly) decoupling scenarios were already found by Reijns in the Higgs sector [6]. I will come back to the scalar sector in the next chapter. However, people have known about the fact that $\overline{MS}$ can break decoupling for a long time. A prominent example can be found in the calculation of the β- function. Remember from section 2.5 that the β-function encodes the dependence of the coupling on the energy scale. To determine the QED β-function, we can investigate the photon self energy again. Instead of using OS-renormalization, we use $\overline{MS}$ to define the counterterm such that it removes the ϵ-pole and the constants (γ_E and $\log(4\pi)$).

To achieve this we take te result of the self-energy calculation (see appendix E.1):

$$i\Pi^{\mu\nu}(q) = i(q^2 g^{\mu\nu} - q^\mu q^\nu)\frac{-8e^2\mu_D^\epsilon}{(4\pi)^{d/2}}\int_0^1 dx\ x(1-x)\frac{\Gamma(2-d/2)}{\Delta^{2-d/2}}\ . \tag{3.17}$$

Next, we use the approximations 2.44-2.47 to expand in terms of ϵ to find:

$$i\Pi^{\mu\nu}(q) = i(q^2 g^{\mu\nu} - q^\mu q^\nu)\frac{-8e^2}{(4\pi)^2}\int_0^1 dx\ x(1-x)\left[\frac{2}{\epsilon} + \log(4\pi) - \gamma_E + \log\left(\frac{\mu_D^2}{\Delta}\right)\right]\ , \tag{3.18}$$

so that the counterterm δ_3 becomes (see appendix C.1):[36]

$$\delta_3 = \frac{-8e^2}{6(4\pi)^2}\left[\frac{2}{\epsilon} + \log(4\pi) - \gamma_E\right]\ . \tag{3.19}$$

Combing the two results in:

$$i\hat{\Pi}^{\mu\nu}(q) = i(q^2 g^{\mu\nu} - q^\mu q^\nu)\frac{8e^2}{(4\pi)^2}\int_0^1 dx\ x(1-x)\log\left(\frac{m^2 - x(1-x)q^2}{\mu_D^2}\right)\ . \tag{3.20}$$

From this we can find the expression for the QED β-function.[37] To this end, one can investigate the observable charge in a scattering experiment. The photon self-energy diagram gives a correction to the charge. The computation of the β-function gives:

$$\beta(e) = \frac{e^3}{12\pi^2}\ . \tag{3.21}$$

Note that this calculation is done in $\overline{MS}$. We can see something interesting happening; the coupling seems to run, no matter the energy scale that is chosen. Even when the energy scale $\mu \ll m$, the coupling still runs. The way that people in the field deal with this is by building in decoupling of heavy particles 'by hand'. In a sense, they define two different β-functions, one for the limit where the energy scale is less than the mass of the particle and one for the limit where the energy scale is higher than the mass of the particle. The β-function 'changes' when a certain threshold is crossed.
The calculation for the β-function can also be done by choosing a Euclidean point ($q^2 = -\mu^2$) and perform OS (or Off-shell) renormalization. From this one finds (see [20]):

$$\beta(e) = \frac{e^3}{2\pi^2}\int_0^1 dx \frac{\mu^2 x^2(1-x)^2}{m^2 + \mu^2 x(1-x)}\ . \tag{3.22}$$

We can investigate two energy limits, firstly when the energy is higher than the mass of the particle in the loop ($\mu > m$):

$$\beta(e) \simeq \frac{e^3}{12\pi^2}\ , \tag{3.23}$$

whereas when the energy is lower one finds:

$$\beta(e) \simeq \frac{e^3}{60\pi^2}\frac{\mu^2}{m^2}\ , \tag{3.24}$$

which explicitly shows decoupling when the energy is much lower than the mass of the particle in the loop. If one does use the $\overline{MS}$-scheme, it is necessary to build in decoupling by hand. If this is not done properly, a poorly behaving perturbative expansion is the result. One can wonder why people still use $\overline{MS}$ despite the requirement of modifying β-functions. The main reason is that calculations are fairly easy using $\overline{MS}$; simply subtract the divergent pole and some constants.

[36] Note that $\int_0^1 dx\ x(1-x) = \frac{1}{6}$.

[37] For the full calculation the reader is referred to [7], [18] or [19]

4 The toy model

In the previous work, done by G. Reijns [6], the implications of a heavy (top) quark in the context of the Higgs self-energy was explored. Specifically, Reijns investigates the behaviour of the self-energy in terms of the heavy (top) mass. He concludes that the (often cited as troublesome) quadratic dependence only occurs when the $\overline{MS}$-renormalization scheme is used. When the OS-scheme is used, the effects are of the order of $\mathcal{O}(\frac{\lambda_t}{m_t}) = \mathcal{O}(m_t^0)$, where m_t is the top mass and λ_t is the Yukawa coupling associated with the top quark. It is also noted that the result does not satisfy the decoupling theorem, as the calculation with internal fermions (i.e. a one-loop correction to the self-energy) is not suppressed with powers of m_t compared to the calculation without internal fermions. This last observation is of course due to the fact that the Yukawa coupling depends on the mass of the particle, a concept already touched upon in chapter 3. In this section, we'd like to explore a (Higgs-like) scalar theory where the coupling with other fields is simply of order $\mathcal{O}(1)$. Based upon the discussion above, we'd expect the self energy to decouple, at least at the one-loop level. If this is the case, can we extend this to all order and for an arbitrary number of external (scalar) legs? This chapter will start with carefully setting up a toy model that has the desired properties. After this, the self energy calculations will be done, followed by an investigation of the Appelquist-Carazzone decoupling theorem. The chapter will end with some 'loose ends', including a discussion on quadratic divergences.

4.1 Setting up the model

As discussed in the previous section, we'd like to set up a scalar toy model. We still want to have a fermion whose mass can be made large, but we do not want the coupling constant to depend on the mass of the fermion. Remember that the reason that, in the SM, the Higgs-fermion coupling depends on the mass is that it *is* the way to give mass to the fermions, see section 2.2.2. We still want a coupling between the fermion and the Higgs[38], but we'd like the coupling not to depend on the mass of the fermion. We cannot simply 'choose' another coupling; this would break the Higgs mechanism, leaving us with no way to give our particles mass. We could, however, construct a toy model in which left- and right-handed fermions are treated equally. We then are allowed to add a mass term 'by hand' in our lagrangian, as this would no longer break gauge-invariance. There is no longer a need for a Higgs field, but we can still add it. For simplicity, we look at a U(1) gauge invariant lagrangian, with *only* a massive top quark and a Higgs field.

$$\mathcal{L}(x) = \bar{\psi} i \not{D} \psi - m\bar{\psi}\psi - \frac{1}{4}(F_{\mu\nu})^2 + \frac{1}{2}(\partial_\mu \phi)^2 - \frac{1}{2}M^2\phi^2 - \frac{\lambda}{4!}\phi^4 - g\bar{\psi}\psi\phi \; . \tag{4.1}$$

Here $D_\mu = \partial_\mu + ieA_\mu(x)$ such that the Lagrangian is U(1) gauge invariant for transformations of the fermion field. Note that we've added the scalar Higgs field with the *opposite* sign for the mass term (as compared to the usual Higgs potential). Also the Higgs does not transform under U(1). Note that, as usual, the mass dimension of the fermion field is 3/2, and the mass dimension of the scalar field is 1. From this we find that we have a dimensionless coupling in the interaction term. To see this, note that the mass dimension of any term in the Lagrangian[39] should be 4, so from the mass terms we can find the dimension of the fields. Knowing these dimensions, the dimension of the coupling can be found from the last term.

From the Lagrangian of equation 4.1 the Feynman rules can be found. These are summarized in appendix C.3. The process of setting up renormalized perturbation theory, described in section 2.4.1 can be repeated for this Lagrangian, leading to extra (counter)terms. These extra terms lead to the counterterm Feynman rules also given in appendix C.3.

[38] In this section and from now on, we'll use 'Higgs' to indicate the Higgs-like scalar particle in this toy model.

[39] The action $S = \int d^4x\mathcal{L}$ is dimensionless, so $[\mathcal{L}] =$ the mass dimension of the Lagrangian $= 4$.

4.2 Self-energy calculations with the toy model

Now that we've set up our Lagrangian, we'll set out to investigate the self energy of our scalar particle. Before investigating the self-energy, we'll have a short discussion on tadpole diagrams. Because we're dealing with a four-point scalar self interaction only, there is no tadpole contribution to the self-energy at the one-loop level. At higher loop order, we could encounter subdiagrams like:

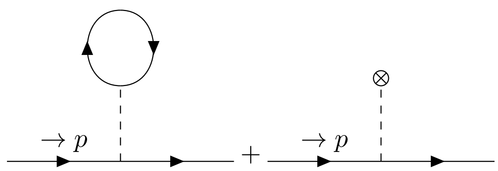

These diagrams are not 1PI and their contribution vanishes when the correct renormalization scheme is used. However, in a general renormalization scheme, the tadpole contribution does not automatically vanish. We would like our theory to be similar to the SM Higgs sector, in which it is imposed that the tadpole counterterm makes the tadpole contribution to the self-energy vanish. This comes from the tadpole renormalization. The reason is that the tadpole diagram adds corrections that are linear in the scalar field, these account for a correction to the vev of the scalar particle. We've now added an extra renormalization condition which states that the vev of the Higgs field should not receive quantum corrections. Diagrammatically we have:

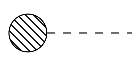 $= 0 \; , \qquad (4.2)$

where the blob indicates 1PI diagrams.

4.2.1 Self-energy

The next step is to calculate the self energy and we'll start with the following diagram:

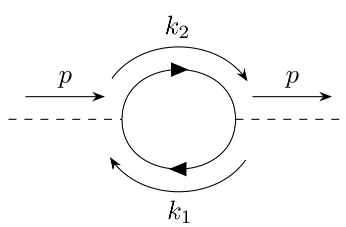

Following the Feynman rules, this diagram corresponds to:

$$
\begin{aligned}
i\Sigma_H^{(1)}(p^2) &= \int \frac{d^4k}{(2\pi)^4}(-1)Tr[(-ig)\frac{i}{\not{k}_2 - m}(-ig)\frac{i}{\not{k}_1 - m}] = \\
&= -g^2 \int \frac{d^4k}{(2\pi)^4} Tr[\frac{\not{k}_2 + m}{k_2^2 - m^2}\frac{\not{k}_1 + m}{k_1^2 - m^2}] \; ,
\end{aligned} \tag{4.3}
$$

where the (-1) originates from the closed fermion loop. Furthermore $k_1 \equiv k$ and $k_2 \equiv k + p$.
The trace works out to be:

$$
Tr[(\not{k}_2 + m)(\not{k}_1 + m)] = 2[(k+p)^2 - m^2 + k^2 - m^2 + 4m^2 - p^2] \; . \tag{4.4}
$$

Next, we apply dimensional regularization:

$$
\begin{aligned}
i\Sigma_H^{(1)}(p^2) =& - g^2\mu_D^\epsilon \int \frac{d^dk}{(2\pi)^d}\frac{2[(k+p)^2-m^2+k^2-m^2+4m^2-p^2]}{[(k+p)^2-m^2][k^2-m^2]} = \\
=& \frac{-ig^2}{16\pi^2}\frac{(2\pi\mu_D)^\epsilon}{i\pi^2}\int d^dk\Big(\frac{2}{k^2-m^2}+\frac{2}{(k+p)^2-m^2}+\frac{8m^2-2p^2}{[(k+p)^2-m^2][k^2-m^2]}\Big) = \\
=& \frac{-ig^2}{16\pi^2}\Big(4A_0(m^2)+(8m^2-2p^2)B_0(p^2,m^2,m^2)\Big)\ .
\end{aligned}
\tag{4.5}
$$

In the last line we've introduced the following shorthand notation for loop integrals:

$$
\begin{aligned}
A_0(m^2) &= \frac{(2\pi\mu_D)^\epsilon}{i\pi^2}\int d^dl\frac{1}{l^2-m^2}\ , \\
B_0(p^2,m_0^2,m_1^2) &= \frac{(2\pi\mu_D)^\epsilon}{i\pi^2}\int d^dl\frac{1}{(l^2-m_0^2)((l+p)^2-m_1^2)}\ .
\end{aligned}
\tag{4.6}
$$

Appendix B.2 provides the expansions for these loop integrals, which are also used in [6] and originate from [21].[40]

Next, we add the counterterms and we find:

$$
i\hat{\Sigma}_{(H)}^{(1)}(p^2) = \frac{-ig^2}{8\pi^2}\Big(2A_0(m^2)+(4m^2-p^2)B_0(p^2,m^2,m^2)\Big) + i[(p^2-M^2)\delta Z_H - \delta M^2]\ . \tag{4.7}
$$

We'll now renormalize this self-energy using the two different renormalization schemes.

4.2.2 OS-Renormalization

First, we'll renormalize using the pole scheme. The two renormalization conditions are:

$$
\begin{aligned}
&1: \hat{\Sigma}_H(p^2=M^2) = 0\ , \\
&2: \frac{d\hat{\Sigma}_H(p^2)}{d(p^2)}\Big|_{p^2=M^2} = 0\ .
\end{aligned}
\tag{4.8}
$$

The first of these conditions leads to:

$$
\delta M^{2,OS} = \frac{-g^2}{8\pi^2}\Big(2A_0(m^2)+(4m^2-M^2)B_0(M^2,m^2,m^2)\Big)\ . \tag{4.9}
$$

For the second, we need the derivative of the self-energy:

$$
i\frac{d\hat{\Sigma}_H(p^2)}{d(p^2)} = \frac{ig^2}{8\pi^2}\Big(-4m^2B_0'(p^2,m^2,m^2)+B_0(p^2,m^2,m^2)+p^2B_0'(p^2,m^2,m^2)\Big)+i\delta Z_H\ . \tag{4.10}
$$

Evaluating this at $p^2 = M^2$ and setting it equal to 0 leads to:

$$
\delta Z_H^{OS} = -\frac{g^2}{8\pi^2}\Big(B_0(M^2,m^2,m^2)-(4m^2-M^2)B_0'(M^2,m^2,m^2)\Big)\ . \tag{4.11}
$$

[40] Note that there is a slightly different definition that is used in [21], they define the dimensional deviation in DREG as $d = 4-2\epsilon$ whereas we use $d = 4-\epsilon$.

So in the OS-scheme, we find:

$$i\hat{\Sigma}^{(1),OS}_{(H)}(p^2) = \frac{-ig^2}{8\pi^2}\Big((4m^2-p^2)B_0(p^2,m^2,m^2) - (4m^2-p^2)B_0(M^2,m^2,m^2) \\ - (p^2-M^2)(4m^2-M^2)B_0'(M^2,m^2,m^2)\Big) \ . \tag{4.12}$$

Next, we'll expand the self energy around $p^2 = M^2$. Due to the renormalization conditions, the first two terms in this expansion evaluate to zero so we'll expand to $\mathcal{O}(p^2-M^2)^2$. The first non-zero term in the expansion is:

$$-\frac{ig^2}{8\pi^2}\Big((4m^2-M^2)B_0''(M^2,m^2,m^2) - 2B_0'(M^2,m^2,m^2)\Big)\frac{1}{2}(p^2-M^2)^2 \tag{4.13}$$

During this expansion we'll explicitly use $p^2 \ll m^2$ as well as $M^2 \ll m^2$ so that it is justified to take the limits of $p^2 \to 0$ and $M^2 \to 0$ in the loop integrals. This allows us to use the approximations provided by Hollik [21]. Later on in this chapter we'll derive the approximations ourselves. The result for the self energy, calculated using the OS scheme is:

$$i\hat{\Sigma}^{(1),OS}_{(H)}(p^2) = \frac{ig^2}{8\pi^2}\frac{(p^2-M^2)^2}{10m^2} \ . \tag{4.14}$$

This result is similar to the result found by Reijns [6], as one might expect. However, we see that now that the coupling does not depend on the mass of the fermion, the self energy does show decoupling: for large values of the fermion-mass, the self energy scales as $1/m^2$.

4.2.3 MS-Renormalization

Next, we'll use the MS-renormalization scheme, with as a starting point equation 4.7. In this scheme the counterterms are required to cancel the divergent parts of the loop integrals so we'll split the loop integrals in a divergent part and a finite part. The self-energy then becomes:

$$i\hat{\Sigma}^{(1)}_{(H)}(p^2) = \frac{-ig^2}{8\pi^2}\Big(2A_0^{div}(m^2) + 2A_0^{fin}(m^2) + (4m^2-p^2)\big[B_0^{div}(p^2,m^2,m^2) + B_0^{fin}(p^2,m^2,m^2)\big]\Big) \\ + i\big((p^2-M^2)\delta Z_H - \delta M^2\big) \ . \tag{4.15}$$

We first cancel the divergent part proportional to p^2, which sets δZ_H:

$$\delta Z_H^{MS} = -\frac{g^2}{8\pi^2}B_0^{div}(p^2,m^2,m^2) \ . \tag{4.16}$$

This in term introduces divergent terms proportional to M^2. The second counter term becomes:

$$\delta M^{2,MS} = -\frac{g^2}{8\pi^2}\Big(2A_0^{div}(m^2) + (4m^2-M^2)B_0^{div}(p^2,m^2,m^2)\Big) \ . \tag{4.17}$$

Substituting these counterterms results in a renormalized self energy given by:

$$i\hat{\Sigma}^{(1),MS}_{(H)}(p^2) = \frac{-ig^2}{8\pi^2}\Big(2A_0^{fin}(m^2) + (4m^2-p^2)B_0^{fin}(p^2,m^2,m^2)\Big) \tag{4.18}$$

Next, this expression is investigated for the heavy quark case, taking the limit of small p^2. Using the expansions for the loop integrals, this expression leads to:

$$\begin{aligned}
i\hat{\Sigma}^{(1),MS}_{(H)}(p^2) &= \frac{-ig^2}{8\pi^2}\Big(2A_0^{fin}(m^2) + 4m^2 B_0^{fin}(0,m^2,m^2) + \\
&\Big[(4m^2-p^2)B_0^{\prime fin}(p^2,m^2,m^2) - B_0^{fin}(p^2,m^2,m^2)\Big]\Big|_{p^2=0}\, p^2 + \\
&\frac{1}{2!}\big[(4m^2-p^2)B_0^{\prime\prime fin}(p^2,m^2,m^2) - 2B_0^{\prime fin}(p^2,m^2,m^2)\big]\Big|_{p^2=0}\, p^4 + \mathcal{O}(p^6)\Big) \\
&= \frac{-ig^2}{8\pi^2}\Big(-2m^2L(m^2) - 4m^2(L(m^2)+1) + [4m^2\frac{1}{6m^2} + L(m^2) + 1]p^2 \\
&+ [\frac{4m^2}{30m^4} - \frac{2}{6m^2}]\frac{p^4}{2} + \mathcal{O}(p^6)\Big) \\
&= \frac{-ig^2}{8\pi^2}\Big(-(6L(m^2)+4)m^2 + [\frac{5}{3} + L(m^2)]p^2 - \frac{1}{10m^2}p^4 + \mathcal{O}(p^6)\Big)\ .
\end{aligned} \tag{4.19}$$

In this expression $L(m^2) = \log\Big(\frac{m^2}{\mu_D^2}\Big) - 1 + \gamma_E - \log(4\pi)$. Here we see that in the calculation of the self energy, using the MS-renormalization scheme, the heavy mass does not decouple. Using the $\overline{MS}$ scheme does not change the overall behaviour of the self-energy in terms of m.

4.2.4 Off-shell renormalization

We see that if we want the decoupling theorem to be satisfied, we'd better use the OS-scheme. The Appelquist-Carazzone decoupling theorem states that *any* low energy renormalization scheme can be used. Let us begin by checking this statement for the self-energy. We'll repeat the renormalization using an Off-Shell scheme, which we'll indicate by OS'. In this section we'll display some intermediate results but full calculation can be found in appendix E.2. We will perform the renormalization at an off-shell point μ (not to be confused with μ_D).[41] The requirement on μ is that the renormalization is performed at a low energy scale, so we require that $\mu \ll m$. The renormalization conditions are similar to that of the OS scheme and are given by:

$$\begin{aligned}
\hat{\Sigma}^{(1)}_H(p^2 = \mu^2) = 0\ , \\
\frac{d\hat{\Sigma}^{(1)}_H(p^2)}{dp^2}\Big|_{p^2=\mu^2} = 0\ .
\end{aligned} \tag{4.20}$$

From these conditions we find that the renormalized self energy in the OS' scheme is given by:

$$\begin{aligned}
i\hat{\Sigma}^{(1),OS'}_{(H)}(p^2) = -\frac{ig^2}{8\pi^2}\Big(&B_0(p^2,m^2,m^2)[4m^2-p^2] + B_0(\mu^2,m^2,m^2)[p^2-4m^2] \\
&+ B_0'(\mu^2,m^2,m^2)\big[p^2(\mu^2-4m^2) - \mu^2(\mu^2-4m^2)\big]\Big)\ .
\end{aligned} \tag{4.21}$$

Performing similar expansions as done before results in:

$$i\hat{\Sigma}^{(1),OS'}_{(H)}(p^2) \approx \frac{ig^2}{8\pi^2}\frac{(p^2-\mu^2)^2}{10m^2}\ , \tag{4.22}$$

which is not a surprising result. In a sense we've just relabeled $M \to \mu$.

[41] As an off-shell point, we use $p^2 = \mu^2$. Sometimes an off-shell Euclidean point is used where $p^2 = -\mu^2$. We've see an example of this in section 3.5.

4.2.5 A change of expansion

Another question that we'll address has to do with the point around which the expansion is done. Up until now, we've expanded the self energy around the same point at which it is performed (M in the OS case and μ in the case of OS'). The result of choosing this expansion point is that the first two terms always vanish as a virtue of the renormalization conditions. We see that when we use OS or OS' renormalization, the first non-zero term is suppressed with powers of the heavy fermion mass m. When we expand around *another* point ξ (which is arbitrary apart from the requirement that $\xi \ll m$) the first two terms will not be zero. It is possible that the shift in expansion point could 'introduce' non-suppressed terms. Furthermore, this non-zero shift in the first two terms will have implications for the full propagator which, in this renormalization scheme, looks like:

$$\frac{i}{p^2 - M^{2,OS'}} + \frac{i}{p^2 - M^{2,OS'}}\big(i\hat{\Sigma}_H^{OS'}(p^2)\big)\frac{i}{p^2 - M^{2,OS'}} + \cdots = \frac{i}{p^2 - M^{2,OS'} + \hat{\Sigma}_H^{OS'}(p^2)} \ . \tag{4.23}$$

The full propagator has a physical pole at

$$p^2 = M^{2,OS} = M^{2,OS'} - \hat{\Sigma}_H^{OS'}(M^{2,OS}) \ . \tag{4.24}$$

The calculation is fairly long and involved. To make this section more readable, the full calculation is given in E.3 and we'll only state intermediate results here. The starting point is the expansion of the renormalized[42] self energy around an arbitrary point ξ:

$$i\hat{\Sigma}^{(1),OS'}_{(H)}(p^2) \approx i\hat{\Sigma}^{(1),OS'}_{(H)}(\xi^2) + \frac{\partial i\hat{\Sigma}^{(1),OS'}_{(H)}(p^2)}{\partial p^2}\Big|_{p^2=\xi^2}(p^2-\xi^2) + \frac{1}{2}\frac{\partial^2 i\hat{\Sigma}^{(1),OS'}_{(H)}(p^2)}{(\partial p^2)^2}\Big|_{p^2=\xi^2}(p^2-\xi^2)^2 \ . \tag{4.25}$$

Each of the terms in this expansion are then investigated. For the derivatives of the loop integrals, the approximations provided by Hollik [21] can be used. However, for the first term in the expansion the difference between the loop integrals is needed. To this end the logarithms in the loop integral are rewritten and expanded around the small parameter $\Delta \equiv 1/\sqrt{1-4m^2/p^2}$. Using this approximation, we can expand the loop integral as:

$$B_0(p^2,m^2,m^2) \approx \frac{2}{\epsilon} - \log\big(\frac{m^2}{\mu_D^2}\big) - \gamma_E + \log(4\pi) + \frac{p^2}{6m^2} + \frac{p^4}{60m^4} + \frac{p^6}{420m^6} + \mathcal{O}(p^8/m^8) + \mathcal{O}(\epsilon) \ . \tag{4.26}$$

From this expression the approximations, provided by Hollik and Reijns, for the derivatives of the loop integrals can easily be extracted. Using these approximations it is found that the first term in the expansion becomes:

$$-\frac{ig^2}{8\pi^2}(\mu^2-\xi^2)\Big(\frac{\xi^2-\mu^2}{10m^2} + \frac{3\xi^4+3\xi^2\mu^2-5\mu^4}{420m^4}\Big) + \mathcal{O}(\epsilon) + \text{more suppressed terms} \ , \tag{4.27}$$

from which it can be seen that all terms are (at least) suppressed with two powers of m.
Similarly, the second term in equation 4.25 results in:

$$\frac{\partial i\hat{\Sigma}^{(1),OS'}_{(H)}(p^2)}{\partial p^2}\Big|_{p^2=\xi^2}(p^2-\xi^2) \approx -\frac{ig^2}{8\pi^2}\Big(\frac{(\mu^2-\xi^2)}{5m^2} + \frac{3(\mu^4-\xi^4)}{140m^4}\Big)(p^2-\xi^2) + \text{more suppressed terms} \ . \tag{4.28}$$

[42] Using OS' renormalization performed at a point $\mu \ll m$.

Lastly, the third term gives:

$$\frac{1}{2}\frac{\partial^2 i\hat{\Sigma}^{(1),OS'}_{(H)}(p^2)}{(\partial p^2)^2}\Big|_{p^2=\xi^2}(p^2-\xi^2)^2 \approx \frac{ig^2}{8\pi^2}\Big(\frac{1}{10m^2}+\frac{3\xi^2}{140m^4}\Big)(p^2-\xi^2)^2 + \text{more suppressed terms} \ . \tag{4.29}$$

So we see that, in all three terms of the expansion, the unavoidable constant shift is suppressed with powers of m. Furthermore, as a cross check, when taking the special case where $\xi = \mu$ it can easily be checked that we return to the earlier found case. From the fact that the shifted terms are suppressed, we can conclude that the pole of the propagator from equation 4.24 looks like:

$$p^2 = M^{2,OS} = M^{2,OS'} - \hat{\Sigma}^{OS'}_H(M^{2,OS}) = M^{2,OS'} + \text{Corrections without fermions} \ , \tag{4.30}$$

because, at first order, the self-energy in the OS'-scheme evaluated at $M^{2,OS}$ is $\frac{-g^2}{8\pi^2}\frac{(M^{2,OS}-M^{2OS'})^2}{10m^2}$. The corrections without fermions come from the 1PI self-energy diagram made possible by the ϕ^4-interaction. Because this correction does not depend on the momentum p^2, its contribution is completely absorbed in the mass renormalization.

So we see that the pole mass and the renormalized mass coincide at first order (apart from suppressed terms). Note that this is even true[43] if $\mu = 0$. The same is true for the residue of the pole. So we conclude that *after renormalization* the heavy fermion is decoupled for *all* low energy renormalizations.

4.2.6 A discussion on the ϵ-expansion

In the calculation of the self energy one of the integrals that appears, has a degree of divergence of two. Given that the idea of dimensional regularization is based on *slightly* deviating from the original four dimensions, one may wonder how legitimate this approach is in this situation. Even if one would allow bigger deviations from four dimensions, in one of the subsequent steps the expressions are expanded around 'small' ϵ. In this section, the self energy is revisited. We work in a general d-dimensional spacetime from the start and will postpone the expansion for small ϵ until the expansion is justified.

Starting off with the expression for the self energy, in d dimensions [44]:

$$i\Sigma^{(1)}_H(p^2) = -g^2\mu_D^\epsilon \int \frac{d^dk}{(2\pi)^d}\Big[\frac{2}{k^2-m^2}+\frac{2}{(k+p)^2-m^2}+\frac{8m^2-2p^2}{((k+p)^2-m^2)(k^2-m^2)}\Big] \ . \tag{4.31}$$

The first two integrals are the same (after shifting the integration variable in the second integral to $l = k+p$). These integrals evaluate to:

$$-2g^2\mu_D^\epsilon \int \frac{d^dk}{(2\pi)^d}\frac{1}{k^2-m^2} = -2g^2\mu_D^\epsilon \frac{-i\Gamma(1-d/2)}{(4\pi)^{d/2}\Gamma(1)}\Big(\frac{1}{m^2}\Big)^{1-d/2} \ . \tag{4.32}$$

The third integral is rewritten using Feynman parameters (see appendix E.4 for the full calculation). The third integral then evaluates to:

$$-g^2\mu_D^\epsilon(8m^2-2p^2)\int \frac{d^dk}{(2\pi)^d}\int_0^1 d\alpha_1 \big[l^2-\Delta(p^2)\big]^{-2} = -g^2\mu_D^\epsilon(8m^2-2p^2)\int_0^1 d\alpha_1 \frac{i\Gamma(2-d/2)}{(4\pi)^{d/2}\Gamma(2)}\Big(\frac{1}{\Delta(p^2)}\Big)^{2-d/2} , \tag{4.33}$$

[43] Renormalizing at $\mu = 0$ is possible in this context because there are no problems with IR divergencies due to massless particles in this theory.

[44] Again, keeping the spinor space in 4 dimensions.

where $\Delta(p^2) \equiv \alpha_1(\alpha_1 - 1)p^2 + m^2$. Next, the counterterms are added and the renormalization conditions set the values of the counterterms. After going through these steps, the renormalized self-energy is given by:

$$
\begin{aligned}
i\hat{\Sigma}_H^{(1)}(p^2) = \frac{2ig^2\mu_D^\epsilon}{(4\pi)^{d/2}} \int_0^1 d\alpha_1 \Big[& -(4m^2)\Gamma(2-d/2)\big\{\big(\frac{1}{\Delta(p^2)}\big)^{2-d/2} - \big(\frac{1}{\Delta(M^2)}\big)^{2-d/2}\big\} \\
& - (p^2)\Gamma(2-d/2)\big\{\big(\frac{1}{\Delta(M^2)}\big)^{2-d/2} - \big(\frac{1}{\Delta(p^2)}\big)^{2-d/2}\big\} \\
& + (p^2 - M^2)(4m^2 - M^2)\Gamma(2-d/2)(d/2-2)\big(\frac{1}{\Delta(M^2)}\big)^{3-d/2}\alpha_1(\alpha_1 - 1)\Big] \, .
\end{aligned}
\tag{4.34}
$$

Now we're in a position where we can expand in terms of ϵ. For the third term, the property of the gamma function $\Gamma(x) = \frac{1}{x}\Gamma(x+1)$ is used. During the expansion some unsuppressed terms appear, but these cancel exactly and all that is left are suppressed terms. As a cross check, the found expression is expanded around $p^2 = M^2$. The zeroth and first order terms vanish, which they should as that is what is imposed by the renormalization conditions. If everything was done correctly, we should find the same expression for the second order term in the expansion as before. The relevant terms are collected from the expansions done on equation 4.34 after which the integral over the Feynman parameter α_1 is performed. The result is:

$$
i\hat{\Sigma}_H^{(1)}(p^2) = \frac{ig^2}{8\pi^2}\frac{(p^2 - M^2)^2}{10m^2} \, , \tag{4.35}
$$

which is indeed the same as the expression found before. So we can conclude that the treatment of loop integrals involving quadratic divergences using DREG is appropriate. The method that we've used here differs slightly from the way we've used it before, but the same result is found which implies that the 'naive' treatment of the dimensional deviation can be done without cause for concern. We can investigate closely what happens (again, see appendix E.4). First of all, as has been mentioned before, when using DREG the quadratic divergence resides in a pole in the Gamma function in two dimensions. We see that this pole is removed upon renormalization. Specifically, the act of taking the derivative creates a term that cancels the pole in the Gamma function. This is comparable to what happened in calculating the photon self energy (E.1).

4.3 The three-point function

In the last section, we've thoroughly investigated the self-energy and it's decoupling properties. Before we move on to the Appelquist-Carazzone theorem, let us consider a diagram with more than two external legs (at the one-loop level). We'll look into the three-point function and we'll slightly simplify the situation by looking at the scenario where the external momenta are of the same order. The diagrams are given by:

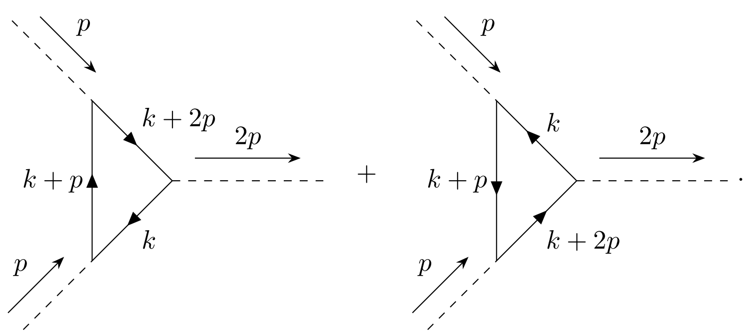

(4.36)

Both diagrams give the same result. The full calculation can be found in appendix E.5. The Feynman rules are followed after which the trace is worked out. Next, the denominator is rewritten using Feynman parameters and a shift in integration variable from $k \to l - \beta p - 2\gamma p$. The shift also causes the numerator to change. All terms in the numerator that are linear in the integration variable l are discarded. The remaining integrals are evaluated using DREG and the result is expanded for small ϵ. After this, the counterterm is added. Note that this is the first time that we've actually *added* a term to the Lagrangian; we did not have a three-point interaction to begin with, so there is no term to split. We'll label the added counterterm by $\lambda_{3,c}$. The renormalization condition that is imposed is:

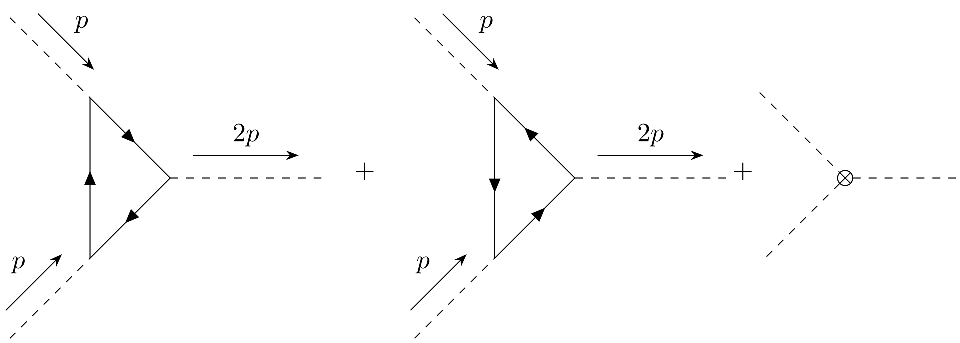

$$= -i\lambda_{3,R} \quad \text{at } p^2 = \mu^2 \ . \tag{4.37}$$

The counterterm diagram is given by $-i\lambda_{3,c}$ and $\lambda_{3,R}$ is the observed (effective) triple scalar coupling. This allows us to find an explicit form for the counterterm ($\lambda_{3,c}$). After all these steps we find that the renormalized three-point function is given by:

$$\frac{ig^3}{(4\pi)^2}\int_0^1 d\beta d\gamma \Big[\underbrace{48m\log\left(\frac{\Delta(p^2)}{\Delta(\mu^2)}\right)}_{1} + \underbrace{\frac{2p^2B}{\Delta(p^2)} - \frac{2\mu^2 B}{\Delta(\mu^2)}}_{2} + \underbrace{8m^3\big(\frac{1}{\Delta(p^2)} - \frac{1}{\Delta(\mu^2)}\big)}_{3}\Big] - i\lambda_{3,R} \ , \tag{4.38}$$

where $\Delta(p^2) \equiv [(\beta+2\gamma)^2 - \beta - 4\gamma]p^2 + m^2$. The next step is to check if the result is indeed suppressed. For the second term it is easy to see, as B depends on one power of m whereas Δ depends on m^2. The first term can be rewritten. We'll introduce the notation $\sigma \equiv (\beta+2\gamma)^2 - \beta - 4\gamma$ to keep the notation uncluttered. We then write:

$$48m\log\left(\frac{\Delta(p^2)}{\Delta(\mu^2)}\right) = 48m\log\left(\frac{\sigma p^2 + m^2}{\sigma\mu^2 + m^2}\right) = 48m\log\left(\frac{m^2(1+\sigma p^2/m^2)}{m^2(1+\sigma\mu^2/m^2}\right) \approx 48\big[\frac{\sigma(p^2-\mu^2)}{m} - \frac{\sigma^2(p^4-\mu^4)}{2m^3} + \dots\big] \ , \tag{4.39}$$

which is indeed suppressed with powers of m. The last term is rewritten as:

$$\begin{aligned} 8m^3\big(\frac{1}{\Delta(p^2)} - \frac{1}{\Delta(\mu^2)}\big) &\approx 8m^3\Big[\frac{1}{m^2}(1 - \frac{\sigma p^2}{m^2} + \frac{\sigma^2 p^4}{m^4} - \dots) - \frac{1}{m^2}(1 - \frac{\sigma\mu^2}{m^2} + \frac{\sigma^2\mu^4}{m^4} - \dots)\Big] = \\ &= \frac{8\sigma(\mu^2 - p^2)}{m} - \frac{8\sigma^2(\mu^4 - p^4)}{m^3} + \dots \ , \end{aligned} \tag{4.40}$$

which is also suppressed. Interestingly, we see that the result after renormalization has the form $(p-\mu) \times \mathcal{O}(\frac{p}{m}, \frac{\mu}{m})$. This is the form that was expected by making use of Lorentz covariance in the Appelquist-Carazzone decoupling theorem in section 3.4. In this case, Lorentz covariance could not be used, but we still find the same structure. The vertex-correction term with mass-dimension 1, proportional to m, disappears in the renormalization process. After renormalization $1/m$-terms remain.

4.4 Appelquist-Carazzone Revisited

In this section we'll revisit the Appelquist-Carazzonne decoupling theorem for our toy model. As was done in chapter 3, we'll start with investigating the degree of divergence in this theory. Let us introduce similar notation as before:

N_h: The number of external scalars;

N_f: The number of external fermions (which is 0);

N_A: The number of external photons (which is 0);

P_h: The number of scalar propagators;

P_f: The number of fermion propagators;

P_γ: The number of photon propagators;

L: The number of loops in the diagram.

The three possible vertices are denoted by:

V: The interaction between a scalar particle and two fermions;

V_4: The quartic scalar coupling;

V_γ: The interaction between a photon and two fermions .

Note that we do not have a three-higgs coupling in our theory. The degree of divergence is given by:

$$D = 4L - P_f - 2P_h - 2P_\gamma \ , \tag{4.41}$$

and the number of vertices is given by:

$$\begin{aligned} 4V_4 + V = N_h + 2P_h \quad &\Rightarrow \quad P_h = 2V_4 + \frac{V}{2} - \frac{N_h}{2} \ , \\ 2V + 2V_\gamma = 2P_f \quad &\Rightarrow \quad V + V_\gamma = P_f \ , \\ V_\gamma = 2P_\gamma \ . & \end{aligned} \tag{4.42}$$

The number of loops is given by:

$$L = V_4 + \frac{V}{2} - \frac{N_h}{2} + \frac{V_\gamma}{2} + 1 \ , \tag{4.43}$$

so for the degree of divergence D we find:

$$D = 4 - N_h \ , \tag{4.44}$$

similar as before. If we were to include a three-point vertex V_3 in our theory, the degree of divergence would depend on the amount of V_3 vertices in the diagram. We will come back to this addition later on in this chapter.

The discussion on the convergent diagrams in section 3.3 depended heavily on the use of $D = 4 - N_b$. Because in our toy model we find the same expression for D; the argument is exactly the same and we can immediately move on to the case of divergent diagrams. Similar to section 3.4, the discussion starts with the renormalization of the diagrams that have $N_h = 2$ and $N_h = 3$. Before, we were able to use the transverse structure of the propagator and the tensor structure of the three-point vertex to reduce the degree of divergence of these diagrams to zero. After this, the counterterm diagrams would lead to a convergent scenario. In the toy model, we cannot use the same methods as there is neither a transverse structure in the scalar propagator nor a tensor structure in the vertices. We've seen in sections 4.2 and 4.3 that we can use the two renormalization conditions to ensure convergent calculations in both cases. The four-point function is logarithmically divergent and can be renormalized similar to how the three-point function was renormalized. There are two differences. First of all, the counterterm for the three-point function had to be *added* to the Lagrangian, as there is no coupling to 'split'. Second of all, the degree of divergence for the four-point vertex is lower.

The four cases that were discussed in section 3.4 can now be investigated in the toy model. The first of these is the scenario where we have divergent parent diagrams and convergent subdiagrams. For this scenario we can use the discussion on the behaviour of convergent subdiagrams and the renormalization of divergent parent diagrams to see that diagrams containing internal fermions are suppressed.

We run into problems when investigating divergent parent diagrams containing divergent subdiagrams. The crucial part in discussing these diagrams was the ability to 'extract' a power of the external momenta from an internal subdiagram. We were able to identify the behaviour of the subdiagram as $k^{4-f} \times$(suppressed terms). This was easy to see due to the tensor structures; when focussing on an internal loop with a tensor structure, the *only* objects that are available to carry that structure are the external momentum and the metric tensor $g^{\mu\nu}$. It would *seem* logical that the behaviour of an internal loop in our toy model will eventually depend on the external momenta multiplied by suppressed terms. This argument is reinforced further by the statement made by Appelquist and Carazzone that the theorem is quite general despite the proof being for a specific model. They do not explicitly state that the argument extends to scalar theories like our toy model. The statement on the behaviour of an internal loop depending only on the external momenta multiplied by suppressed terms has been checked in the cases of $N_h = f$. We cannot easily extend this argument, however, to the most general case.

4.5 The three-point interaction

As has been touched upon in section 4.3, we do not have a triple-scalar interaction in our theory and the counterterm for the three-point function had to be added to the lagrangian. In the SM, the Higgs has a triple physical Higgs interaction. We can modify the toy model to resemble the SM Higgs sector a bit more by allowing a new interaction term in the Lagrangian given by:

$$\Delta\mathcal{L}(x) = -\frac{\lambda_3}{3!}\phi^3 \; . \tag{4.45}$$

The extra vertex allows for extra (self-energy) diagrams in our calculations. The one-loop diagram that is added will not introduce powers of the fermion mass and will not be considered. The main difference comes from the discussion on the degree of divergence. The steps are the same as taken in section 3.2 but the dependence on the three-point vertex does not cancel. The result is given by:

$$D = 4 - N_h - V_3 \; , \tag{4.46}$$

where V_3 indicates the amount of triple-scalar vertices in the diagram. Luckily, we see that every extra V_3 *reduces* the degree of divergence by one. This makes it possible to repeat the entire argument for the cases $V_3 = 1, 2, 3$, after which we're always in the scenario of convergent parent diagrams.

5 Conclusion & Outlook

This work has looked at the decoupling properties of renormalizable theories. It began with a careful investigation of the Appelquist-Carazzone decoupling theorem in the scenario of a particular gauge theory in chapter 3. Part of the argument of the decoupling theorem depended on the degree of divergence found by powercounting. In this argument it was important that we're dealing with 1PI diagrams, so that deviations in the degree of divergence are not present, a concept explored in section 2.3.1. In the case of more general diagrams, the tensor structure of the propagators and vertices was used to simplify the argument. It allowed us to identify external momenta as factors of a divergent internal fermion loop. The rest of the factors stemming from the fermion loop are suppressed by factors of m in the large mass limit and after *proper* renormalization. The act of properly renormalizing a diagram means that the subtractions are performed at a low energy scale μ. To explicitly see decoupling, we need $\mu \ll m$ in the large mass limit. A known example of a scenario where the use of the $\overline{MS}$ renormalization scheme 'breaks' decoupling properties was discussed in section 3.5.

In chapter 4 a toy model involving a scalar particle and a (heavy) fermion was introduced. In the calculation of the self energy of the scalar particle, it was shown that decoupling properties can be observed, provided a proper renormalization scheme was used. It was explicitly seen that the use of MS/$\overline{MS}$ does not result in a decoupling scenario. It seems that the use of such a renormalization scheme 'mixes' the scales which we're trying to separate. The use of on-shell or even off-shell renormalization with adequate renormalization conditions results in a decoupling scenario. It was explicitly checked that there is no dependence on the expansion point of the self-energy (which is often chosen as the same point as the renormalization point). If we expand the self energy around the same point as where we renormalize, the first two terms in the expansion automatically vanish due to the renormalization conditions. Choosing another point to expand (which is still small compared to m) causes the first two terms to acquire a non-zero shift. It was shown in section 4.2.5 that this shift is finite and terms that have an m-dependence all have a negative power of m. From this calculation we've seen that, after renormalization, the heavy fermion decouples for *all* low energy renormalizations. This is even true when we choose to renormalize at $\mu = 0$. The discussion on self-energies in the toy model ended with an investigation on the validity of using DREG for quadratic divergencies. It was shown in section 4.2.6 that, provided we work in a general d-dimensional spacetime from the start, we can delay the expansion in the 'small' parameter ϵ, representing the departure from four dimensions, until after renormalization. This ensures that the parameter in which we expand can indeed be taken as a small parameter. During this calculation, the quadratic divergence shows up as a pole in the Gamma function in two dimensions. It was shown that this pole cancels during the renormalization procedure, leaving behind a pole in four dimensions for which ϵ can be used as an expansion parameter.

In section 4.3 the three-point function that appears at the one-loop level was renormalized in the toy model. After renormalization the decoupling properties can be seen from the fact that the resulting expression depends on negative powers of the fermion mass. During this calculation, the required counterterms had to be added to the Lagrangian, as there was no three-point interaction term present in the original Lagrangian. If the degree of divergence of effective n-point vertices would not decrease with increasing n, an infinite amount of extra terms would have to be added to the Lagrangian. In the toy model that we've constructed this is not the case, for every extra external scalar particle the degree of divergence is lowered by one.

In section 4.4 the Appelquist-Carazzone decoupling theorem was revisited in the context of our toy model. We've seen that part of the argument can be immediately applied to the toy model. The second part of the argument became more troublesome. In the toy model, we neither have a tensor structure in our vertices nor do we have a transverse structure in our propagators. This causes the argument to become more difficult to generalize to arbitrarily high loop order. Specifically, we cannot assume that we can extract powers of the

external momenta from our internal diagram, after which the only factors that are left are suppressed[45] with powers of m. Explicit decoupling has been shown for the cases where the amount of legs of the subdiagram is equal to the amount of external scalar particles.
The fact that we can apply the reasoning of Appelquist & Carazzone to our toy model (at least for a limited number of diagrams) does have interesting implications. First of all it further supports the conclusions drawn by Reijns [6], who goes into the dependence of the renormalization scheme used in the context of self-energy diagrams involving scalar particles. We've seen, more generally, that *if* we would like the decoupling theorem to hold; we need to apply renormalization at a low energy scale. Furthermore, our discussion extended to diagrams with more than two external legs. Decoupling properties can also be 'broken' by looking at renormalizable theories where the coupling depends on the mass of the heavy particle. In this case all calculations involving heavy particles bring with them extra factors of the heavy mass. We see that this also causes energy scales to be mixed, however the use of proper renormalization makes the (heavy) mass dependence much less catastrophic than most literature would suggest.

5.1 Outlook

As stated before, we believe the argument of Appelquist and Carazzone can be further applied to the scenario of our toy model and more general models involving scalar particles. Future research could investigate the method of extending the argument for more general loops. One possibility is to look into a recursive argument, where one begins in (one of) the 'inner' loops in a general diagram. Including counterterms step by step, it is possible to go outwards from this subdiagram. If one can show that the momentum dependence can be linked to the external momenta[46], then it can be linked to the argument of Appelquist and Carazzone. This would extend the argument of this thesis to *all* orders in perturbation theory. If the argument on general diagrams is to be applied to models including scalar particles, it becomes exceedingly important to make sure that energy scales stay separated. The use of $\overline{MS}$ seems to 'mix' the high-energy scales with the low ones. In performing higher-order calculations, one also needs to consider the different energy scales of the integrals. It might be possible to achieve this by splitting the integral in different regions and performing the integration 'shell by shell'.

Another interesting extension to our toy model is a model where we have multiple scalar particles. This is relevant in the context of Grand Unified Theories (GUT's), but brings along further complications. The difficulty that such a model brings when investigating the decoupling theorem lies in the powercounting. There seems to be no easy argument to determine the degree of divergence without a strong dependence on the inner structure of the diagram.

Lastly, an interesting extension could be found in exploring the link between this work and the Callan-Symanzik equation and/or the work done by Mooij and Shaposhnikov, who studied a finite, divergence free approach to renormalization[22]. They also apply their theory to ϕ^4 theory and then do look into the case of multiple scalars, rather than heavy fermions.

[45] After renormalization.
[46] And suppressed terms otherwise.

Appendices

Appendix A List of Abbreviations

1PI	One-particle Irreducible
DoF	Degree of freedom
DREG	Dimensional Regularization
EFT	Effective Field Theory
IR	Infrared
MS	Minimal Subtraction
$\overline{MS}$	Modified Minimal Subtraction
OS	On-Shell
OS'	Off-Shell
QCD	Quantum Chromodynamics
QED	Quantum Electrodynamics
QFT	Quantum Field Theory
QGC	Quartic Gauge Coupling
QM	Quantum Mechanics
RGE	Renormalization Group Equation
SSB	Spontaneous Symmetry Breaking
SM	Standard Model
SO	Special Orthogonal
SU	Special Unitary
TGC	Triple Gauge Coupling
UV	Ultraviolet
vev	Vacuum Expectation Value
YM	Yang-Mills

Appendix B List of integrals

B.1 Standard integrals

Here we quote the results of some d-dimensional loop integrals in Minkowski space, often encountered in Feynman diagrams:

$$\int \frac{d^d l}{(2\pi)^d} \frac{1}{(l^2 - \Delta)^n} = \frac{(-1)^n i}{(4\pi)^{d/2}} \frac{\Gamma(n - \frac{d}{2})}{\Gamma(n)} \Big(\frac{1}{\Delta}\Big)^{n-\frac{d}{2}} \tag{B.1}$$

$$\int \frac{d^d l}{(2\pi)^d} \frac{l^2}{(l^2 - \Delta)^n} = \frac{(-1)^{n-1} i}{(4\pi)^{d/2}} \frac{d}{2} \frac{\Gamma(n - \frac{d}{2} - 1)}{\Gamma(n)} \Big(\frac{1}{\Delta}\Big)^{n-\frac{d}{2}-1} \tag{B.2}$$

B.2 Notation for one-loop integrals

In this section, the (commonly used) notation for the loop integrals is summarized. We follow the notation used by [6], which in term follows [21].

The one-loop tadpole diagram corresponds to:

$$A_0(m^2) = \frac{(2\pi\mu_D)^\epsilon}{i\pi^2} \int d^d l \frac{1}{l^2 - m^2} \ , \tag{B.3}$$

and the one-loop two point scalar integral reads:

$$B_0(p^2, m_0^2, m_1^2) = \frac{(2\pi\mu_D)^\epsilon}{i\pi^2} \int d^d l \frac{1}{(l^2 - m_0^2)((l+p)^2 - m_1^2)} \tag{B.4}$$

Hollik et al provide us with useful expansions of these integrals [21]:

$$A_0(0) = 0, \tag{B.5a}$$

$$A_0(m^2) = \frac{2m^2}{\epsilon} - m^2 L(m^2) + \mathcal{O}(\epsilon), \tag{B.5b}$$

$$B_0(0, m^2, m^2) = (1 - \frac{\epsilon}{2}) \frac{A_0(m^2)}{m^2}, \tag{B.5c}$$

$$B_0(m^2, 0, m^2) = \frac{2}{\epsilon} + 1 - L(m^2) + \mathcal{O}(\epsilon), \tag{B.5d}$$

$$B_0'(0, 0, 0) = 0, \tag{B.5e}$$

$$B_0'(0, 0, m^2) = \frac{1}{2m^2} + \mathcal{O}(\epsilon), \tag{B.5f}$$

$$\tag{B.5g}$$

where:

$$\begin{aligned} L(m^2) &= log(\frac{m^2}{\mu_D^2}) - C \\ C &= 1 - \gamma_E + log(4\pi) \end{aligned} \tag{B.6}$$

Appendix C Feynman Rules

C.1 QED

In this section, the Feynman rules for QED in renormalized perturbation theory are summarized.

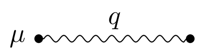

$$\leftrightarrow \frac{-ig_{\mu\nu}}{q^2 + i\eta} \ ;$$

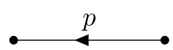

$$\leftrightarrow \frac{i(\not{p} + m)}{p^2 - m^2 + i\eta} \ ;$$

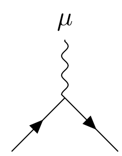

$$\leftrightarrow -ie\gamma^\mu \ ;$$

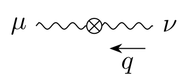

$$\leftrightarrow -i(g^{\mu\nu} q^2 - q^\mu q^\nu)\delta_3 \ ; \tag{C.1}$$

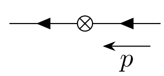

$$\leftrightarrow i(\not{p}\delta_2 - \delta m) \ ;$$

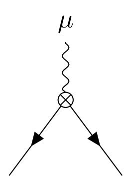

$$\leftrightarrow -ie\gamma^\mu \delta_1 \ .$$

The counterterm for the one-loop correction to the fermion propagator has a more complicated form in chiral theories. In this case the Feynman rule for the counterterm is:

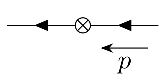

$$\leftrightarrow i[\not{p}(\delta Z_{f_L} P_L + \delta Z_{f_R} P_R) - \frac{1}{2} m_f (\delta Z_{f_L} + \delta Z_{f_R}) - \delta m_f] \ , \tag{C.2}$$

which reduces to the form given above when dealing with a non chiral theory in which $Z_{f_L} = Z_{f_R} = Z_f$.

C.2 QCD

Here we'll state the relevant QCD Feynman rules. The only relevant rules in the context of this thesis are the rules for the TGC and the QGC. These are given by:

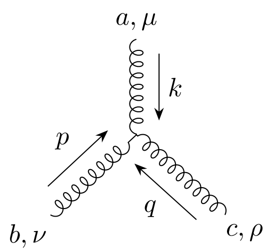

$$\leftrightarrow g f^{abc}\big[g^{\mu\nu}(k-p)^{\rho} + g^{\nu\rho}(p-q)^{\mu} + g^{\rho\mu}(q-k)^{\nu}\big] \ . \tag{C.3}$$

and

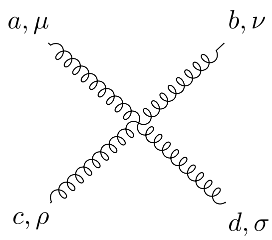

$$\leftrightarrow \quad -ig^2\big[f^{abe}f^{cde}(g^{\mu\rho}g^{\nu\sigma} - g^{\mu\sigma}g^{\nu\rho}) + f^{ace}f^{bde}(g^{\mu\nu}g^{\rho\sigma} - g^{\mu\sigma}g^{\nu\rho}) + f^{ade}f^{bce}(g^{\mu\nu}g^{\rho\sigma} - g^{\mu\rho}g^{\nu\sigma})\big] \ . \tag{C.4}$$

C.3 Toy model

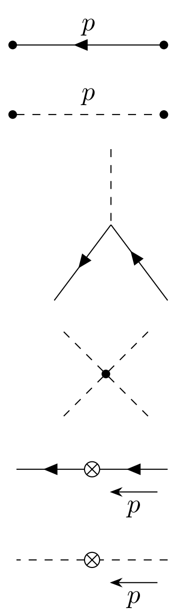

$$\leftrightarrow \frac{i(\not{p}+m)}{p^2-m^2+i\eta} \ ;$$
$$\leftrightarrow \frac{i}{p^2-M^2+i\eta} \ ;$$
$$\leftrightarrow -ig \ ;$$
$$\leftrightarrow -i\lambda \ ;$$
$$\leftrightarrow i(\not{p}\delta_2 - \delta m) \ ;$$
$$\leftrightarrow i[(p^2-M^2)\delta Z_H - \delta M^2] \ . \tag{C.5}$$

The gauge boson part is not needed in this thesis.

Appendix D Miscellaneous Mathematics

D.1 Feynman Parameters

In loop integrals, there are often multiple (different) denominators. It is easier to work with one denominator raised to some power. The way to 'squeeze' multiple denominators into one denominator-structure is by the method of Feynman parameters. Let's start with a simple example where we have two factors in the denominator:

$$\begin{aligned}\frac{1}{AB} &= \frac{1}{A-B}\left(\frac{1}{B}-\frac{1}{A}\right) = \left[\frac{1}{A-B}\frac{1}{yB+(1-y)A}\right]_{y=0}^{y=1} = \\ &= \int_0^1 dy \frac{1}{[yB+(1-y)A]^2} = \int_0^1 dx \int_0^1 dy \delta(x+y-1)\frac{1}{[xA+yB]^2} \ .\end{aligned} \tag{D.1}$$

This can be extended to arbitrarily complicated denominator structures:

$$\prod_{j=1}^{n} \frac{1}{a_j^{\nu_j}} = \frac{\Gamma(\Sigma_j \nu_j)}{\Pi_j \Gamma(\nu_j)} \int_0^1 \frac{\prod_j (dx_j x_j^{\nu_j - 1})\delta(1-\Sigma_j x_j)}{\left(x_1 a_1 + x_2 a_2 + \cdots + x_n a_n\right)^{\Sigma_j \nu_j}} \quad , \nu_j \text{ a positive integer} \ . \tag{D.2}$$

Equation D.2 can be proven by first applying mathematical induction to go from equation D.1 to a similar equation with n denominators and then repeatedly differentiating the resulting expression to get the different powers ν_j.

D.2 Dirac Algebra

When doing calculations involving fermions, we often encounter traces of products of n gamma matrices ($n \in \mathbb{N}$). In this section, some useful trace-identities will be introduced. Remember that we've introduced the gamma matrices as:

$$\{\gamma^\mu, \gamma^\nu\} = \gamma^\mu\gamma^\nu + \gamma^\nu\gamma^\mu = 2g^{\mu\nu}\mathbb{1} \ . \tag{D.3}$$

As stated in the introduction, an explicit representation (called the Weyl representation) is often used. In this representation the Dirac matrices are:

$$\gamma^0 = \begin{pmatrix} 0 & \mathbb{1}_2 \\ \mathbb{1}_2 & 0 \end{pmatrix}, \quad \gamma^k = \begin{pmatrix} 0 & \sigma^k \\ -\sigma^k & 0 \end{pmatrix}, \quad \gamma^5 = \begin{pmatrix} -\mathbb{1}_2 & 0 \\ 0 & \mathbb{1}_2 \end{pmatrix} \tag{D.4}$$

with the Pauli spin matrices given by:

$$\sigma^1 = \begin{pmatrix} 0 & 1 \\ 1 & 0 \end{pmatrix} \ , \ \sigma^2 = \begin{pmatrix} 0 & -i \\ i & 0 \end{pmatrix} \ , \ \sigma^3 = \begin{pmatrix} 1 & 0 \\ 0 & -1 \end{pmatrix} \ . \tag{D.5}$$

To derive some of the properties of (traces of) gamma matrices, let us also introduce a useful product of gamma matrices:

$$\gamma^5 = i\gamma^0\gamma^1\gamma^2\gamma^3 \ . \tag{D.6}$$

This product has the property that $(\gamma^5)^2 = \mathbb{1}$ and $\{\gamma^\mu, \gamma^5\} = 0$. The first trace identity is for $n = 0$: $\mathrm{Tr}\{\mathbb{1}\} = 4$.
Next, let us investigate the trace of one gamma matrix:

$$\mathrm{Tr}\,\gamma^\mu = \mathrm{Tr}\,\gamma^5\gamma^5\gamma^\mu = -\,\mathrm{Tr}\,\gamma^5\gamma^\mu\gamma^5 = -\,\mathrm{Tr}\,\gamma^5\gamma^5\gamma^\mu = -\,\mathrm{Tr}\,\gamma^\mu \ , \tag{D.7}$$

where, in the third step, we've used the cyclic property of traces. From this we see that this trace is equal to itself with a minus sign, hence $\mathrm{Tr}\{\gamma^\mu\} = 0$. This method can be extended to the trace of n gamma matrices. Here the γ^5 has to be anti-commuted n times to the right, so the trace of n gamma matrices vanishes if n is odd. Next, we look at the trace of two gamma matrices, using the defining property:

$$\mathrm{Tr}\,\gamma^\mu\gamma^\nu = \mathrm{Tr}(2g^{\mu\nu}1 - \gamma^\nu\gamma^\mu) = 8g^{\mu\nu} - \mathrm{Tr}\,\gamma^\mu\gamma^\nu \ . \tag{D.8}$$

So $\mathrm{Tr}\,\gamma^\mu\gamma^\nu = 4g^{\mu\nu}$. By repeating this trick, traces of longer products of (an even amount of) gamma matrices can be found. In summary, some of the useful trace identities read

$$\begin{aligned} \mathrm{Tr}(\mathbb{1}) &= 4 \ , \\ \mathrm{Tr}(\text{odd nr of } \gamma\text{'s}) &= 0 \ , \\ \mathrm{Tr}(\gamma^\mu\gamma^\nu) &= 4g^{\mu\nu} \ , \\ \mathrm{Tr}(\gamma^\mu\gamma^\nu\gamma^\rho\gamma^\sigma) &= 4(g^{\mu\nu}g^{\rho\sigma} - g^{\mu\rho}g^{\nu\sigma} + g^{\mu\sigma}g^{\nu\rho}) \end{aligned} \tag{D.9}$$

It is also useful to know how to deal with contracted gamma matrices. For example:

$$\gamma^\mu\gamma_\mu = g_{\mu\nu}\gamma^\mu\gamma^\nu = \frac{1}{2}g_{\mu\nu}\{\gamma^\mu, \gamma^\nu\} = g_{\mu\nu}g^{\mu\nu} = 4 \ . \tag{D.10}$$

Using the anti-commutation relation, we can also find:

$$\begin{aligned} \gamma^\mu\gamma^\nu\gamma_\mu &= -2\gamma^\nu \\ \gamma^\mu\gamma^\nu\gamma^\rho\gamma_\mu &= 4g^{\nu\rho} \ . \end{aligned} \tag{D.11}$$

In $d = 4 - \epsilon$ dimensions these contraction identities change to:

$$\begin{aligned} \gamma^\mu\gamma^\nu\gamma_\mu &= -(2-\epsilon)\gamma^\nu \ , \\ \gamma^\mu\gamma^\nu\gamma^\rho\gamma_\mu &= 4g^{\nu\rho} - \epsilon\gamma^\nu\gamma^\rho \end{aligned} \tag{D.12}$$

D.3 Lie groups and Lie algebras

Throughout the theory, the working example has been QED. QED is a U(1) gauge theory, where the group U(1) is an Abelian group. Later we've talked about non-Abelian gauge theories. In this section we'll provide a little more background in the language of group theory and the ideas of Lie groups. We'll start with the axioms of a group.
A group is a combination of a set and an operation $\cdot$. The operation combines two elements of the set to form a new element. The combination of the set and operation is called a group if it satisfies all of the following four group axioms:

- $(G1)$ Closure: if $g_1 \in G$ and $g_2 \in G$ then $g_1 \cdot g_2 \in G$.
- $(G2)$ Associativity: if g_1, g_2 and g_3 are in G, then $g_1 \cdot (g_2 \cdot g_3) = (g_1 \cdot g_2) \cdot g_3$.
- $(G3)$ Identity: There is an identity element e in G, such that $e \cdot g = g \cdot e$ for all $g \in G$.
- $(G4)$ Inverse: for all $g \in G$ there is an inverse $g^{-1} \in G$ such that $g \cdot g^{-1} = g^{-1} \cdot g = e$.

In particle physics a special type of group, called the Lie group, is particularly important. Lie groups are groups that are parametrized by continuous variables. In the $U(1)$ example that we've already seen the variable is encoded in the phase $\exp\{i\alpha(x)\}$. Continuously generated groups can have elements arbitrarily close to the identity element. From this fact it follows that *any* group element can be reached by the repeated action of infinitesimal elements. The infinitesimal elements can be written as:

$$g(\alpha) = \mathbb{1} + i\alpha^a T^a + \mathcal{O}(\alpha^2), \tag{D.13}$$

where the coefficients of the parameters α^a are Hermitian operators.[47] These coefficients, T^a are called the *generators* of the group.
An important property of the generators is that they must span the space of (infinitesimal) group transformations. The vector space that is spanned by the generators of the Lie group is called the *Lie algebra*. It follows that the commutator of the generators can be written as a linear combination of generators:

$$\left[T^a, T^b\right] = i f^{abc} T^c, \tag{D.14}$$

where f^{abc} are the *structure constants*.
The important groups in particle physics are the special unitary (SU) and the special orthogonal (SO) groups. The group SU(N) is the set of $N \times N$ matrices that are unitary [48] and have determinant equal to one. The group SO(N) is the set of $N \times N$ matrices that are orthogonal[49] and have determinant equal to one.

Appendix E Long Calculations

E.1 The photon self-energy

In this appendix, the full calculation for the photon self energy is written out. The calculation closely follows steps taken in [7]. The photon self-energy at one-loop order is given by the diagram:

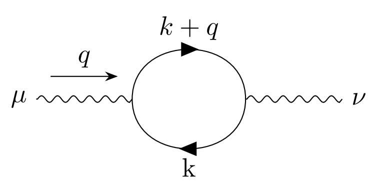

Figure 10: Photon self-energy diagram.

Following the Feynman rules, this diagram results in:

$$(-ie)^2(-1)\int \frac{d^4k}{(2\pi)^4}\,\mathrm{Tr}\left[\gamma^\mu \frac{i}{\not{k}-m}\gamma^\nu \frac{i}{\not{k}+\not{q}-m}\right] \equiv i\Pi^{\mu\nu}(q)\ , \tag{E.1}$$

We'll start with calculating the trace, so we look at:

$$\begin{aligned}&\mathrm{Tr}\left[\gamma^\mu(\not{k}+m)\gamma^\nu(\not{k}+\not{q}+m)\right] = \mathrm{Tr}\left[\gamma^\mu\not{k}\gamma^\nu\not{k}\right] + \mathrm{Tr}\left[\gamma^\mu\not{k}\gamma^\nu\not{q}\right] + \mathrm{Tr}\left[\gamma^\mu m\gamma^\nu m\right] = \\ &= 8k^\mu k^\nu - 4k^2 g^{\mu\nu} + 4k^\mu q^\nu - 4k\cdot q g^{\mu\nu} + 4k^\nu q^\mu + 4m^2 g^{\mu\nu}\ .\end{aligned} \tag{E.2}$$

For the denominator, we'll use Feynman parameters:

$$\frac{1}{(k^2-m^2)((k+q)^2-m^2)} = \int_0^1 dx \frac{1}{(k^2+2xk\cdot q + xq^2 - m^2)^2} = \int_0^1 dx \frac{1}{(l^2-\Delta)^2}\ , \tag{E.3}$$

[47] A Hermitian operator H is defined by the property that it is its own Hermitian conjugate i.e. $H^\dagger = H$.
[48] A unitary matrix U has the property that $U^\dagger U = UU^\dagger = \mathbb{1}$.
[49] An orthogonal matrix U has the property that $U^T U = UU^T = \mathbb{1}$.

with $\Delta \equiv m^2 - x(1-x)q^2$ and l=k+xq. The shift in integration coordinate causes the numerator to become:

$$
\begin{aligned}
&8l^\mu l^\nu - 8xl^\mu q^\nu - 8xl^\nu q^\mu + 8x^2 q^\mu q^\nu - 4(l^2 - 2xl\cdot q + x^2q^2)g^{\mu\nu} + 4l^\mu q^\nu - 4xq^\mu q^\nu - 4(l\cdot q - xq^2)g^{\mu\nu} \\
&+ 4l^\nu q^\mu - 4xq^\mu q^\nu + 4m^2 g^{\mu\nu} = \\
&= 4\Big(2l^\mu l^\nu - g^{\mu\nu}l^2 - 2x(1-x)q^\mu q^\nu + g^{\mu\nu}(m^2 + x(1-x)q^2)\Big) + (\text{linear terms in l}) \ .
\end{aligned} \tag{E.4}
$$

The terms linear in l will evaluate to 0 upon integration and are therefore not written out.
So the expression for the self-energy becomes:

$$
-4e^2\mu_D^\epsilon \int_0^1 dx \int \frac{d^dl}{(2\pi)^d}\Big(\frac{2l^\mu l^\nu - g^{\mu\nu}l^2 - 2x(1-x)q^\mu q^\nu + g^{\mu\nu}(m^2 + x(1-x)q^2)}{(l^2-\Delta)^2}\Big) \ , \tag{E.5}
$$

where DREG has been applied. The first two terms can be combined into quadratic terms (in l) by using $l^\mu l^\nu \to \frac{1}{d}l^2 g^{\mu\nu}$. Let us investigate this (possibly troublesome[50]) term first:

$$
\begin{aligned}
-(1-\frac{2}{d})g^{\mu\nu}\int \frac{d^dl}{(2\pi)^d}\frac{l^2}{(l^2-\Delta)^2} &= -(1-\frac{2}{d})g^{\mu\nu}\Big(\frac{(-i)}{(4\pi)^{d/2}}\frac{d}{2}\frac{\Gamma(2-d/2-1)}{\Gamma(2)}\big(\frac{1}{\Delta}\big)^{2-d/2-1}\Big) = \\
&= \frac{i}{(4\pi)^{d/2}}\Gamma(2-d/2)\big(\frac{1}{\Delta}\big)^{2-d/2}\big(-\Delta g^{\mu\nu}\big) \ ,
\end{aligned} \tag{E.6}
$$

where the property of the Gamma-function $\Gamma(x+1) = x\Gamma(x)$ was used in the second step to write:

$$
(1-\frac{2}{d})\frac{d}{2}\Gamma(1-d/2) = \frac{(-1)(1-d/2)}{(1-d/2)}\Gamma(2-d/2) \ .
$$

Next, we look at the remaining integrals:

$$
\begin{aligned}
&\Big[g^{\mu\nu}(m^2 + x(1-x)q^2) - 2x(1-x)q^\mu q^\nu\Big]\int \frac{d^dl}{(2\pi)^d}\frac{1}{l^2-\Delta)^2} = \\
=&\Big[g^{\mu\nu}(m^2 + x(1-x)q^2) - 2x(1-x)q^\mu q^\nu\Big]\frac{i}{(4\pi)^{d/2}}\Gamma(2-d/2)\big(\frac{1}{\Delta}\big)^{2-d/2}
\end{aligned} \tag{E.7}
$$

So the self-energy is given by:

$$
\begin{aligned}
i\Pi^{\mu\nu}(q) = &-4ie^2\mu_D^\epsilon \int_0^1 dx \frac{1}{(4\pi)^{d/2}}\frac{\Gamma(2-d/2)}{\Delta^{2-d/2}}\times \\
&\Big(g^{\mu\nu}(-\Delta) + g^{\mu\nu}(m^2 + x(1-x)q^2) - 2x(1-x)q^\mu q^\nu\Big) = \\
&= (q^2 g^{\mu\nu} - q^\mu q^\nu)\cdot i\Pi(q^2) \ ,
\end{aligned} \tag{E.8}
$$

with

$$
\Pi(q^2) = \frac{-8e^2\mu_D^\epsilon}{(4\pi)^{d/2}}\int_0^1 dx \ x(1-x)\frac{\Gamma(2-d/2)}{\Delta^{2-d/2}} \ . \tag{E.9}
$$

We see that we can indeed extract the structure, as 'predicted' by the Ward identity. Furthermore, we see that, when using DREG, the Ward identity stays valid and the quadraticly divergent integral does not cause problems. It was not necessary to expand around $d = 4$ to show this.

[50] Note, $D = 2$ in this case!

E.2 Off-shell renormalization of the self-energy

In this section, the full calculation of the Higgs self-energy in the toy model will be given. The starting point of this calculation is the expression for the self-energy as given in equation 4.7, which reads:

$$i\hat{\Sigma}^{(1)}_{(H)}(p^2) = \frac{-ig^2}{8\pi^2}\Big(2A_0(m^2) + (4m^2 - p^2)B_0(p^2, m^2, m^2)\Big) + i[(p^2 - M^2)\delta Z_H - \delta M^2] \ . \tag{E.10}$$

The renormalization conditions now read:

$$\begin{aligned} &\hat{\Sigma}^{(1)}_H(p^2 = \mu^2) = 0 \ , \\ &\frac{d\hat{\Sigma}^{(1)}_H(p^2)}{dp^2}\Big|_{p^2=\mu^2} = 0 \ . \end{aligned} \tag{E.11}$$

Starting with the second condition, we find:

$$\frac{d\hat{\Sigma}^{(1)}_H(p^2)}{dp^2}\Big|_{p^2=\mu^2} = -\frac{ig^2}{8\pi^2}\Big((4m^2 - \mu^2)B_0'(\mu^2, m^2, m^2) - B_0(\mu^2, m^2, m^2)\Big) + i\delta Z_H^{OS'} = 0 \ , \tag{E.12}$$

from which we can read off the wavefunction renormalization counterterm:

$$i\delta Z_H^{OS'} = -\frac{ig^2}{8\pi^2}\Big(B_0(\mu^2, m^2, m^2) - (4m^2 - \mu^2)B_0'(\mu^2, m^2, m^2)\Big) \ . \tag{E.13}$$

The mass counterterm is then found by looking at the first renormalization condition. For this we find:

$$i\delta M^{2,OS'} = -\frac{ig^2}{8\pi^2}\Big(2A_0(m^2)+(4m^2-\mu^2)B_0(\mu^2, m^2, m^2)+(\mu^2-M^2)[B_0(\mu^2, m^2, m^2)-(4m^2-\mu^2)B_0'(\mu^2, m^2, m^2)]\Big) \ . \tag{E.14}$$

So that the final expression for the self energy is:

$$\begin{aligned} i\hat{\Sigma}^{(1),OS'}_{(H)}(p^2) = -\frac{ig^2}{8\pi^2}\Big(&B_0(p^2, m^2, m^2)[4m^2 - p^2] + B_0(\mu^2, m^2, m^2)[p^2 - 4m^2] \\ &+ B_0'(\mu^2, m^2, m^2)\big[p^2(\mu^2 - 4m^2) - \mu^2(\mu^2 - 4m^2)\big]\Big) \ . \end{aligned} \tag{E.15}$$

We can check that this indeed vanishes at $p^2 = \mu^2$, furthermore if we choose $\mu^2 = M^2$ we recover the expression found earlier. Next we expand the self energy around the renormalization point μ^2:

$$i\hat{\Sigma}^{(1),OS'}_{(H)}(p^2) \approx i\hat{\Sigma}^{(1),OS'}_H(\mu^2) + \frac{\partial i\hat{\Sigma}^{(1),OS'}_{(H)}(p^2)}{\partial p^2}\Big|_{p^2=\mu^2}(p^2 - \mu^2) + \frac{1}{2}\frac{\partial^2 i\hat{\Sigma}^{(1),OS'}_{(H)}(p^2)}{(\partial p^2)^2}\Big|_{p^2=\mu^2}(p^2 - \mu^2)^2 \ . \tag{E.16}$$

The first two terms in this expansion evaluate to zero, by virtue of the renormalization conditions. The expansion thus results in:

$$i\hat{\Sigma}^{(1),OS'}_{(H)}(p^2) \approx \frac{-ig^2}{8\pi^2}\big[B_0''(\mu^2, m^2, m^2)(4m^2 - \mu^2) - 2B_0'(\mu^2, m^2, m^2)\big]\frac{1}{2}(p^2 - \mu^2)^2 \ . \tag{E.17}$$

Using the approximations for the large m limit and expanding the (derivatives of the) loop integrals for $\mu^2 \ll m^2$ results in:

$$i\hat{\Sigma}^{(1),OS'}_{(H)}(p^2) \approx \frac{ig^2}{8\pi^2}\frac{(p^2 - \mu^2)^2}{10m^2} \ . \tag{E.18}$$

This result is not surprising, in a sense we've just relabeled $M \to \mu$.

E.3 Self-energy expansion around another point

In this section, the full calculation for the expansion of the self-energy at an arbitrary point ξ is worked out. This is done to check that there are no terms that scale with positive powers of m in the first two terms of the expansion. When expanding around the same point at which the renormalization was performed, the first two terms always evaluate to zero. The expansion, around a point labeled by $\xi \ll m$ is given by:

$$i\hat{\Sigma}^{(1),OS'}_{(H)}(p^2) \approx i\hat{\Sigma}^{(1),OS'}_{(H)}(\xi^2) + \frac{\partial i\hat{\Sigma}^{(1),OS'}_{(H)}(p^2)}{\partial p^2}\Big|_{p^2=\xi^2}(p^2-\xi^2) + \frac{1}{2}\frac{\partial^2 i\hat{\Sigma}^{(1),OS'}_{(H)}(p^2)}{(\partial p^2)^2}\Big|_{p^2=\xi^2}(p^2-\xi^2)^2 \ . \quad \text{(E.19)}$$

We'll investigate each of these terms separately.

The first term
The first term is:

$$-\frac{ig^2}{8\pi^2}\Big(\big[B_0(\xi^2,m^2,m^2)-B_0(\mu^2,m^2,m^2)\big](4m^2-\xi^2)+B_0'(\mu^2,m^2,m^2)[\xi^2(\mu^2-4m^2)-\mu^2(\mu^2-4m^2)]\Big) \ . \quad \text{(E.20)}$$

We can approximate this using the fact that $\xi^2 \ll m^2$ and $\mu^2 \ll m^2$. The second part (proportional to $B_0'(\mu^2,m^2,m^2)$) then becomes:

$$B_0'(\mu^2,m^2,m^2)(4m^2-\mu^2)(\mu^2-\xi^2) \approx 2/3(\mu^2-\xi^2) - \frac{\mu^2}{30m^2}(\mu^2-\xi^2) - \frac{\mu^4}{210m^4}(\mu^2-\xi^2) + \dots \quad \text{(E.21)}$$

Next the first terms are investigated, specifically:
$[B_0(\xi^2,m^2,m^2) - B_0(\mu^2,m^2,m^2)](4m^2-\xi^2)$. To this end the difference between the loop integrals must be considered. Starting off with the relevant expression for the loop integral (with $m_1 = m_2$) we have[21]:

$$B_0(p^2,m^2,m^2) = \frac{2}{\epsilon} + \Big\{1 - L(m^2) + \frac{R}{2p^2}\big[\log\big(2m^2-p^2+R\big) - \log\big(2m^2-p^2-R\big)\big]\Big\} + \mathcal{O}(\epsilon) \ , \quad \text{(E.22)}$$

where (in the case that $m_1 = m_2$):

$$\begin{aligned} R &= \sqrt{p^4 - 4m^2p^2} \ , \\ L(m^2) &= \log\left(\frac{m^2}{\mu_D^2}\right) - C \ , \\ C &= 1 - \gamma_E + \log(4\pi) \ . \end{aligned} \quad \text{(E.23)}$$

Note that inside the logarithm, the μ_D is the parameter introduced by dimensional regularization, not the subtraction scale.
We'll begin by finding an approximation for the logarithms:

$$\begin{aligned} &\frac{R}{2p^2}\log\Big(\frac{2m^2-p^2+\sqrt{p^4-4m^2p^2}}{2m^2-p^2-\sqrt{p^4-4m^2p^2}}\Big) = \frac{\sqrt{1-4m^2/p^2}}{2}\log\Big(\frac{2m^2/p^2-1+\sqrt{1-4m^2/p^2}}{2m^2/p^2-1-\sqrt{1-4m^2/p^2}}\Big) = \\ &= \sqrt{1-4m^2/p^2}\log\Big(\frac{\sqrt{1-4m^2/p^2}-1}{\sqrt{1-4m^2/p^2}+1}\Big) = \frac{1}{\Delta}\log\Big(\frac{1-\Delta)}{1+\Delta)}\Big) = \frac{1}{\Delta}\Big(\log(1-\Delta) - \log(1+\Delta)\Big) \ , \end{aligned} \quad \text{(E.24)}$$

where in the second step, $2m^2/p^2 - 1 + \sqrt{1-4m^2/p^2}$ was rewritten as $(-1/2)(\sqrt{1-4m^2/p^2}-1)^2$ and a similar term for the denominator. The factors of $-1/2$ cancel and the square is taken out of the log, which cancels the factor $1/2$.
In the third step we've factored out a factor of $\sqrt{1-4m^2/p^2}$ and defined $\Delta \equiv 1/\sqrt{1-4m^2/p^2}$. We've now arrived at a form that can be expanded in the small parameter Δ:

$$\begin{aligned}\frac{1}{\Delta}\Big(\log(1-\Delta)-\log(1+\Delta)\Big) &\approx \frac{1}{\Delta}\Big(-\Delta-\frac{\Delta^2}{2}-\frac{\Delta^3}{3}-\dots-(\Delta-\frac{\Delta^2}{2}+\frac{\Delta^3}{3}-\dots)\Big) = \\ &= -2-\frac{2\Delta^2}{3}-\frac{2\Delta^4}{5}+\mathcal{O}(\Delta^6)\ .\end{aligned} \tag{E.25}$$

The compact, full form reads:

$$\frac{1}{\Delta}\Big(\log(1-\Delta)-\log(1+\Delta)\Big) = -2\sum_{n=0}^{\infty}\frac{\Delta^{2n}}{(2n+1)}\ . \tag{E.26}$$

Applying this approximation to expression E.22:

$$\begin{aligned}B_0(p^2,m^2,m^2) &\approx \frac{2}{\epsilon}-\log\big(\frac{m^2}{\mu_D^2}\big)-\gamma_E+\log(4\pi)-\frac{2}{3}\Delta^2-\frac{2}{5}\Delta^4-\frac{2}{7}\Delta^6+\mathcal{O}(\Delta^8)+\mathcal{O}(\epsilon)\\ &\approx \frac{2}{\epsilon}-\log\big(\frac{m^2}{\mu_D^2}\big)-\gamma_E+\log(4\pi)+\Big(\frac{p^2}{6m^2}+\frac{p^4}{24m^4}+\frac{p^6}{96m^6}\Big)-\Big(\frac{p^4}{40m^4}+\frac{p^6}{80m^6}\Big)\\ &+\frac{p^6}{224m^6}+\mathcal{O}(p^8/m^8)+\mathcal{O}(\epsilon)\\ &= \frac{2}{\epsilon}-\log\big(\frac{m^2}{\mu_D^2}\big)-\gamma_E+\log(4\pi)+\frac{p^2}{6m^2}+\frac{p^4}{60m^4}+\frac{p^6}{420m^6}+\mathcal{O}(p^8/m^8)+\mathcal{O}(\epsilon)\ .\end{aligned} \tag{E.27}$$

We've purposefully gone to order p^6, because here we can recognise the earlier used approximations for higher order derivatives of the loop integral.
Now, what does this imply for equation E.20? Recall that we were investigating:

$$\begin{aligned}[B_0(\xi^2,m^2,m^2)-B_0(\mu^2,m^2,m^2)](4m^2-\xi^2) &\approx \Big(\frac{2}{\epsilon}-\log\Big(\frac{m^2}{\mu_D^2}\Big)-\gamma_E+\log(4\pi)+\frac{\xi^2}{6m^2}+\frac{\xi^4}{60m^4}+\frac{\xi^6}{420m^6}+\mathcal{O}(\xi^8/m^8)\\ &-\frac{2}{\epsilon}+\log\big(\frac{m^2}{\mu_D^2}\big)+\gamma_E-\log(4\pi)-\frac{\mu^2}{6m^2}-\frac{\mu^4}{60m^4}-\frac{\mu^6}{420m^6}+\mathcal{O}(\mu^8/m^8)\Big)\\ &(4m^2-\xi^2)+\mathcal{O}(\epsilon)\\ &=\frac{2}{3}(\xi^2-\mu^2)-\frac{\xi^2}{6m^2}(\xi^2-\mu^2)+\frac{1}{15m^2}(\xi^4-\mu^4)\\ &-\frac{\xi^2}{60m^4}(\xi^4-\mu^4)+\frac{1}{105m^4}(\xi^6-\mu^6)+\mathcal{O}(\epsilon)+\text{more suppressed terms}\ .\end{aligned} \tag{E.28}$$

In this expression, it would seem that potential troublesome terms might appear in which the powers in the numerator are not equal to the powers of m in the denominator. However, we have to factor out the term $(\mu^2-\xi^2)$ such that the coefficient multiplying it is dimensionless and suppressed.
So the first term in our expansion becomes:

$$-\frac{ig^2}{8\pi^2}(\mu^2-\xi^2)\Big(\frac{\xi^2-\mu^2}{10m^2}+\frac{3\xi^4+3\xi^2\mu^2-5\mu^4}{420m^4}\Big)+\mathcal{O}(\epsilon)+\text{more suppressed terms}\ , \tag{E.29}$$

from which we see that the first term in our expansion is suppressed with powers of m.

Second term
The second term in the expansion is given by:

$$\frac{\partial i\hat{\Sigma}^{(1),OS'}_{(H)}(p^2)}{\partial p^2}\Big|_{p^2=\xi^2}(p^2-\xi^2) = -\frac{ig^2}{8\pi^2}\Big(B_0'(\xi^2,m^2,m^2)(4m^2-\xi^2) - B_0'(\mu^2,m^2,m^2)(4m^2-\mu^2) + B_0(\mu^2,m^2,m^2) - B_0(\xi^2,m^2,m^2)\Big)(p^2-\xi^2)\ . \tag{E.30}$$

For the first of these terms, the approximation for the derivative of the loop integral in the high mass limit is used:

$$\begin{aligned} B_0'(\xi^2,m^2,m^2)(4m^2-\xi^2) - B_0'(\mu^2,m^2,m^2)(4m^2-\mu^2) \approx &(\frac{1}{6m^2}+\frac{\xi^2}{30m^4}+\frac{\xi^4}{140m^6}+\dots)(4m^2-\xi^2) \\ &-(\frac{1}{6m^2}+\frac{\mu^2}{30m^4}+\frac{\mu^4}{140m^6}+\dots)(4m^2-\mu^2) = \\ &= \frac{\mu^2-\xi^2}{30m^2}+\frac{\mu^4-\xi^4}{210m^4}+\mathcal{O}(\frac{\mu^6}{m^6},\frac{\xi^6}{m^8})\ . \end{aligned} \tag{E.31}$$

The second terms are evaluated by using the approximation E.27 and give:

$$\frac{\mu^2-\xi^2}{6m^2}+\frac{\mu^4-\xi^4}{60m^4}+\dots \tag{E.32}$$

So, the entire second term in the expression gives:

$$\frac{\partial i\hat{\Sigma}^{(1),OS'}_{(H)}(p^2)}{\partial p^2}|_{p^2=\xi^2}(p^2-\xi^2) \approx -\frac{ig^2}{8\pi^2}\Big(\frac{(\mu^2-\xi^2)}{5m^2}+\frac{3(\mu^4-\xi^4)}{140m^4}\Big)(p^2-\xi^2) + \text{more suppressed terms}\ . \tag{E.33}$$

Third term
The third term is given by:

$$\begin{aligned} \frac{1}{2}\frac{\partial^2 i\hat{\Sigma}^{(1),OS'}_{(H)}(p^2)}{(\partial p^2)^2}\Big|_{p^2=\xi^2}(p^2-\xi^2)^2 \approx &-\frac{ig^2}{8\pi^2}\Big(B_0''(\xi^2,m^2,m^2)(4m^2-\xi^2) - 2B_0'(\xi^2,m^2,m^2)\Big)\frac{1}{2}(p^2-\xi^2)^2 = \\ &\approx -\frac{ig^2}{8\pi^2}\Big[(\frac{1}{30m^4}+\frac{\xi^2}{70m^6})(4m^2-\xi^2) - (\frac{2}{6m^2}+\frac{2\xi^2}{30m^4})\Big]\frac{1}{2}(p^2-\xi^2)^2 = \\ &= \frac{ig^2}{8\pi^2}\Big(\frac{1}{10m^2}+\frac{3\xi^2}{140m^4}\Big)(p^2-\xi^2)^2 + \text{more suppressed terms}\ . \end{aligned} \tag{E.34}$$

So we see that, in all three terms of the expansion, the unavoidable constant shift is suppressed with powers of m. Furthermore, as a cross check, when taking the special case where $\xi = \mu$ it can easily be checked that we return to the earlier found case.

E.4 Self energy revisited

In the calculation of the self energy one of the integrals that appears, has a degree of divergence of two. Given that the idea of dimensional regularization is based on *slightly* deviating from the original four dimensions, one may wonder how legitimate this approach is in this situation. Even if one would allow bigger deviations from four dimensions, in one of the subsequent steps the expressions are expanded around 'small' ϵ. In this section, the self energy is revisited. We work in a general d-dimensional spacetime from the start and will postpone the expansion for small ϵ until the expansion is justified.
Starting off with the expression for the self energy, in d dimensions [51]:

$$i\Sigma_H^{(1)}(p^2) = -g^2\mu_D^\epsilon \int \frac{d^dk}{(2\pi)^d}\Big[\frac{2}{k^2-m^2} + \frac{2}{(k+p)^2-m^2} + \frac{8m^2-2p^2}{((k+p)^2-m^2)(k^2-m^2)}\Big] \ . \tag{E.35}$$

The first of these integrals:

$$-2g^2\mu_D^\epsilon \int \frac{d^dk}{(2\pi)^d}\frac{1}{k^2-m^2} = -2g^2\mu_D^\epsilon \frac{-i\Gamma(1-d/2)}{(4\pi)^{d/2}\Gamma(1)}\big(\frac{1}{m^2}\big)^{1-d/2} \ . \tag{E.36}$$

The second integral is the same after shifting the integration variable to $l = k + p$.
The third integral is:

$$-g^2\mu_D^\epsilon(8m^2-2p^2)\int \frac{d^dk}{(2\pi)^d}\frac{1}{[(k+p)^2-m^2](k^2-m^2)} \ , \tag{E.37}$$

which is rewritten using Feynman parameters as:

$$\begin{aligned}\int \frac{d^dk}{(2\pi)^d}\frac{1}{[(k+p)^2-m^2](k^2-m^2)} &= \int \frac{d^dk}{(2\pi)^d}\int_0^1 d\alpha_1 d\alpha_2\big[\alpha_1[(k+p)^2-m^2]+\alpha_2[k^2-m^2]\big]^{-2}\delta(\alpha_1+\alpha_2-1)\\ &= \int \frac{d^dk}{(2\pi)^d}\int_0^1 d\alpha_1\big[k^2+2k\cdot(\alpha_1 p)+\alpha_1 p^2-m^2\big]^{-2}\\ &= \int \frac{d^dl}{(2\pi)^d}\int_0^1 d\alpha_1\big[l^2-\Delta(p^2)\big]^{-2} \ ,\end{aligned} \tag{E.38}$$

where in the last step a shift in integration variable $l = k + \alpha_1 p$ is introduced.

Here $\Delta(p^2) \equiv \alpha_1(\alpha_1-1)p^2 + m^2$, where the momentum dependence has been explicitly stated to keep the notation clear during the process of renormalization. With this, our third integral can be evaluated:

$$-g^2\mu_D^\epsilon(8m^2-2p^2)\int \frac{d^dl}{(2\pi)^d}\int_0^1 d\alpha_1\big[l^2-\Delta(p^2)\big]^{-2} = -g^2\mu_D^\epsilon(8m^2-2p^2)\int_0^1 d\alpha_1\frac{i\Gamma(2-d/2)}{(4\pi)^{d/2}\Gamma(2)}\big(\frac{1}{\Delta}\big)^{2-d/2} \ . \tag{E.39}$$

So the (unrenormalized) self energy is given by:[52]

$$i\Sigma_H^{(1)}(p^2) = \frac{2ig^2\mu_D^\epsilon}{(4\pi)^{d/2}}\int_0^1 d\alpha_1\Big[2\Gamma(1-d/2)\big(\frac{1}{m^2}\big)^{1-d/2} - (4m^2-p^2)\Gamma(2-d/2)\big(\frac{1}{\Delta}\big)^{2-d/2}\Big] \ . \tag{E.40}$$

[51] Again, keeping the spinor space in 4 dimensions.

[52] It can be argued that the first two integrals require a different ϵ than the third, also causing a different ϵ in the exponent of the parameter μ_D. This point will be addressed shortly.

Next, the counterterms are added and we apply the OS-renormalization conditions, the first of which sets the mass counterterm as:

$$\delta M^{2,OS} = \frac{2g^2\mu_D^\epsilon}{(4\pi)^{d/2}}\int_0^1 d\alpha_1\Big[2\Gamma(1-d/2)\big(\frac{1}{m}\big)^{1-d/2} - (4m^2-M^2)\Gamma(2-d/2)\big(\frac{1}{\Delta(M^2)}\big)^{2-d/2}\Big] \ , \tag{E.41}$$

after which we're left with:

$$i\hat{\Sigma}_H^{(1)}(p^2) = \frac{2ig^2\mu_D^\epsilon}{(4\pi)^{d/2}}\int_0^1 d\alpha_1\Big[-(4m^2-p^2)\Gamma(2-d/2)\big(\frac{1}{\Delta(p^2)}\big)^{2-d/2} + (4m^2-M^2)\Gamma(2-d/2)\big(\frac{1}{\Delta(M^2)}\big)^{2-d/2}\Big] \\ + i(p^2-M^2)\delta Z_H \ . \tag{E.42}$$

From the mass counterterm, it can be seen that the imprudence with the (possibly) different ϵ's does not matter, as the first two integrals are cancelled by the mass counterterm, in which the same distinction in ϵ's can be made. To determine the wave function renormalization counterterm, the derivative is required. For this, we also need:

$$\frac{\partial}{\partial(p^2)}\big(\frac{1}{\Delta(p^2)}\big)^{2-d/2} = (d/2-2)\big(\frac{1}{\Delta(p^2)}\big)^{3-d/2}\alpha_1(\alpha_1-1) \ , \tag{E.43}$$

and we find:

$$\delta Z_H^{OS} = \frac{2g^2\mu_D^\epsilon}{(4\pi)^{d/2}}\int_0^1 d\alpha_1\Big[-\Gamma(2-d/2)\big(\frac{1}{\Delta(M^2)}\big)^{2-d/2} + (4m^2-M^2)\Gamma(2-d/2)(d/2-2)\big(\frac{1}{\Delta(M^2)}\big)^{3-d/2}\alpha_1(\alpha_1-1)\Big] \ . \tag{E.44}$$

So the renormalized self energy is:

$$\begin{aligned} i\hat{\Sigma}_H^{(1)}(p^2) = \frac{2ig^2\mu_D^\epsilon}{(4\pi)^{d/2}}\int_0^1 d\alpha_1\Big[&-(4m^2-p^2)\Gamma(2-d/2)\big(\frac{1}{\Delta(p^2)}\big)^{2-d/2} + (4m^2-M^2)\Gamma(2-d/2)\big(\frac{1}{\Delta(M^2)}\big)^{2-d/2} \\ &+ (p^2-M^2)\Big\{-\Gamma(2-d/2)\big(\frac{1}{\Delta(M^2)}\big)^{2-d/2} \\ &+ (4m^2-M^2)\Gamma(2-d/2)(d/2-2)\big(\frac{1}{\Delta(M^2)}\big)^{3-d/2}\alpha_1(\alpha_1-1)\Big\}\Big] \\ = \frac{2ig^2\mu_D^\epsilon}{(4\pi)^{d/2}}\int_0^1 d\alpha_1\Big[&-(4m^2)\Gamma(2-d/2)\big\{\big(\frac{1}{\Delta(p^2)}\big)^{2-d/2} - \big(\frac{1}{\Delta(M^2)}\big)^{2-d/2}\big\} \\ &-(p^2)\Gamma(2-d/2)\big\{\big(\frac{1}{\Delta(M^2)}\big)^{2-d/2} - \big(\frac{1}{\Delta(p^2)}\big)^{2-d/2}\big\} \\ &+ (p^2-M^2)(4m^2-M^2)\Gamma(2-d/2)(d/2-2)\big(\frac{1}{\Delta(M^2)}\big)^{3-d/2}\alpha_1(\alpha_1-1)\Big] \ . \end{aligned} \tag{E.45}$$

Now we will investigate each of the three terms individually by expanding in terms of ϵ. The first term:

$$\begin{aligned} &-\frac{\mu_D^\epsilon}{(4\pi)^{d/2}}(4m^2)\Gamma(2-d/2)\big\{\big(\frac{1}{\Delta(p^2)}\big)^{2-d/2} - \big(\frac{1}{\Delta(M^2)}\big)^{2-d/2}\big\} = \\ &= -(1+\epsilon\log(\mu_D))\frac{4m^2}{(4\pi)^2}(1+\frac{\epsilon}{2}\log(4\pi))(\frac{2}{\epsilon}-\gamma_E)\big\{1-\frac{\epsilon}{2}\log\big(\Delta(p^2)\big) - 1 + \frac{\epsilon}{2}\log\big(\Delta(M^2)\big)\big\} = \\ &= -\frac{4m^2}{(4\pi)^2}\log\bigg(\frac{\Delta(M^2)}{\Delta(p^2)}\bigg) + \mathcal{O}(\epsilon) \ . \end{aligned} \tag{E.46}$$

We can investigate the behaviour in terms of m^2 by rewriting and expanding the logarithm. To keep the notation from getting too cluttered, we define $\beta \equiv \alpha_1(\alpha_1 - 1)$:

$$\begin{aligned} -4m^2 \log\left(\frac{\Delta(M^2)}{\Delta(p^2)}\right) &= -4m^2 \log\left(\frac{1+\beta M^2/m^2}{1+\beta p^2/m^2}\right) \approx -(4m^2)(\frac{\beta M^2}{m^2} - \frac{\beta^2 M^4}{2m^4} + \dots - \frac{\beta p^2}{m^2} + \frac{\beta^2 p^4}{2m^4} - \dots) = \\ &= -4\big[\beta(M^2 - p^2) + \frac{\beta^2(p^4 - M^4)}{2m^2} + \dots\big] \ . \end{aligned} \tag{E.47}$$

We see that everything (except for the first term) is suppressed in terms of m.

The second term is the same with $4m^2 \to p^2$ and an extra minus sign:

$$\frac{p^2}{(4\pi)^2} \log\left(\frac{\Delta(M^2)}{\Delta(p^2)}\right) + \mathcal{O}(\epsilon) \ , \tag{E.48}$$

which is suppressed:

$$p^2 \log\left(\frac{\Delta(M^2)}{\Delta(p^2)}\right) \approx \frac{p^2}{m^2}\Big[\beta(M^2 - p^2) + \frac{\beta^2(p^4 - M^4)}{2m^2} + \dots\Big]. \tag{E.49}$$

For the third term, we use the property of the gamma function $\Gamma(x) = \frac{1}{x}\Gamma(x+1)$ to write:

$$\begin{aligned} &+ (p^2 - M^2)(4m^2 - M^2)\Gamma(3 - d/2)\frac{1}{(2-d/2)}(d/2 - 2)\frac{1}{\Delta(M^2)}\big(\frac{1}{\Delta(M^2)}\big)^{2-d/2}\alpha_1(\alpha_1 - 1) = \\ &= -(p^2 - M^2)(4m^2 - M^2)\frac{\alpha_1(\alpha_1 - 1)}{\Delta(M^2)}(1 - \frac{\epsilon\gamma_E}{2})(1 - \frac{\epsilon}{2}\log\big(\Delta(M^2)\big) = \\ &= -(p^2 - M^2)(4m^2 - M^2)\frac{\alpha_1(\alpha_1 - 1)}{\Delta(M^2)} + \mathcal{O}(\epsilon) \ . \end{aligned} \tag{E.50}$$

This term can be written as;

$$\begin{aligned} -(p^2 - M^2)(4m^2)(1 - \frac{M^2}{4m^2})\frac{\beta}{\beta M^2 + m^2} &= -(p^2 - M^2)(4\beta)\frac{1 - M^2/(4m^2)}{1 + \beta M^2/m^2} \\ &\approx -(p^2 - M^2)(4\beta)\big(1 - \frac{\beta M^2}{m^2} + \frac{\beta^2 M^4}{m^4} - \dots\big)(1 - \frac{M^2}{4m^2}) \ . \end{aligned} \tag{E.51}$$

We see that the non-suppressed term cancels with the non-suppressed term found earlier. So we conclude that the heavy mass decouples when using this alternative method.
As a cross check,we can compare the $(p^2 - M^2)^2$-term with the earlier found expression 4.14. Collecting terms of this order from the expansions done above gives:

$$-\frac{ig^2}{8\pi^2}\frac{(p^2 - M^2)^2}{m^2}\int_0^1 d\alpha_1\big[2\alpha_1^2(\alpha_1 - 1)^2 + \alpha_1(\alpha_1 - 1)\big] = \frac{ig^2}{8\pi^2}\frac{(p^2 - M^2)^2}{10m^2} \ , \tag{E.52}$$

which is indeed the same as the expression found before.

E.5 Renormalization of the three-point function

In this section we will renormalize the three-point function in the toy model. To simplify calculations a little bit, we'll look at the case where the external momenta are of the same order. The diagrams are given by:

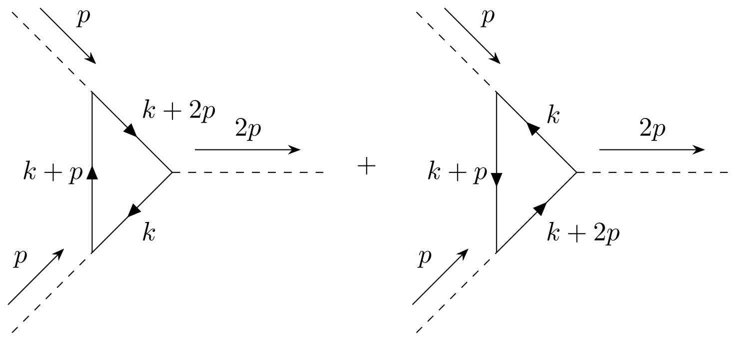

(E.53)

Both diagrams give the same result.

Following the Feynman rules leads to:

$$-2g^3\int\frac{d^4k}{(2\pi)^4}\,\mathrm{Tr}\left\{\frac{(\not{k}+m)(\not{k}+2\not{p}+m)(\not{k}+\not{p}+m)}{(k^2-m^2)[(k+p)^2-m^2][(k+2p)^2-m^2]}\right\}\ , \tag{E.54}$$

where the trace evaluates to:

$$\mathrm{Tr}\big\{(\not{k}+m)(\not{k}+2\not{p}+m)(\not{k}+\not{p}+m)\big\} = 12mk^2+24m(k\cdot p)+8mp^2+4m^3\ . \tag{E.55}$$

The denominator will be rewritten using Feynman parameters. The result, after shifting the integration variable $k\to l-\beta p-2\gamma p$ is:

$$\big((k^2-m^2)[(k+p)^2-m^2][(k+2p)^2-m^2]\big)^{-1} = 2\int_0^1 d\beta d\gamma\big[l^2-\Delta(p^2)\big]^{-3}\ , \tag{E.56}$$

where $\Delta(p^2)\equiv[(\beta+2\gamma)^2-\beta-4\gamma]p^2+m^2$ and the factor of 2 comes from the gamma function in equation D.2. The shift in the integration variable also changes the numerator, which becomes:

$$12ml^2+A\cdot l+Bp^2+4m^3\ , \tag{E.57}$$

where

$$\begin{aligned}A &= -24m(\beta p+2\gamma p)+24mp\ ,\\ B &= 12m\big[(\beta+2\gamma)^2-2\beta-4\gamma+2/3\big]\ .\end{aligned} \tag{E.58}$$

So the integral has been rewritten as:

$$-4g^3\int_0^1 d\beta d\gamma\int\frac{d^4k}{(2\pi)^4}\frac{12ml^2+A\cdot l+Bp^2+4m^3}{(l^2-\Delta(p^2))^3}\ . \tag{E.59}$$

The 'A-part' vanishes upon integration and will be left out from now on. The remaining three integrals will be considered separately. The first integral is UV-divergent and therefore requires DREG:

$$-4g^3\int_0^1 d\beta d\gamma\int\frac{d^4k}{(2\pi)^4}\frac{12ml^2}{(l^2-\Delta(p^2))^3} = \frac{-48ig^3m}{(4\pi)^2}\int_0^1 d\beta d\gamma\Big[\frac{2}{\epsilon}+\log\Big(\frac{\mu_D^2}{\Delta(p^2)}\Big)-\gamma_E+\log(4\pi)-\frac{1}{2}+\mathcal{O}(\epsilon)\Big]\ . \tag{E.60}$$

The second integral yields:

$$-4g^3\int_0^1 d\beta d\gamma\int\frac{d^4k}{(2\pi)^4}\frac{Bp^2}{(l^2-\Delta(p^2))^3}=\frac{+2ig^3}{(4\pi)^2}\int_0^1 d\beta d\gamma Bp^2\frac{1}{\Delta(p^2)}\ . \tag{E.61}$$

The last integral is similar:

$$-4g^3\int_0^1 d\beta d\gamma\int\frac{d^4k}{(2\pi)^4}\frac{4m^3}{(l^2-\Delta(p^2))^3}=\frac{2ig^3}{(4\pi)^2}4m^3\int_0^1 d\beta d\gamma\frac{1}{\Delta(p^2)}\ . \tag{E.62}$$

Next, we impose a renormalization condition by adding a counterterm to the Lagrangian and demanding that:

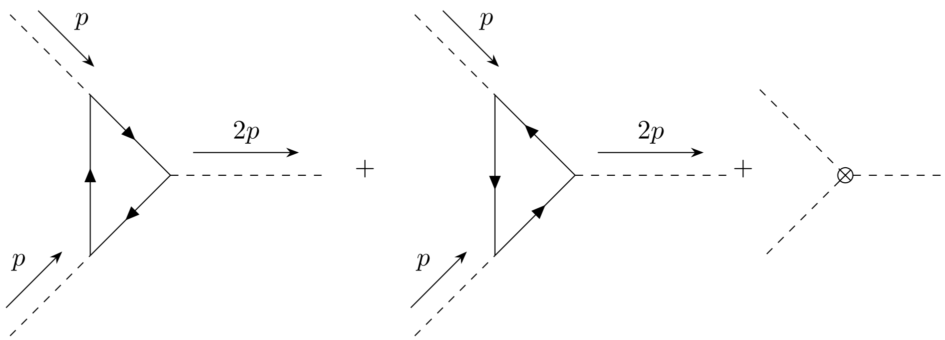

$$= -i\lambda_{3,R} \qquad \text{at } p^2=\mu^2\ . \tag{E.63}$$

The counterterm diagram is given by $-i\lambda_{3,c}$ and $\lambda_{3,R}$ is the observed (effective) triple scalar coupling. From this renormalization condition it follows that the counterterm ($\lambda_{3,c}$) is given by:

$$i\lambda_{3,c}=i\lambda_{3,R}+\frac{ig^3}{(4\pi)^2}\int_0^1 d\beta d\gamma\Big\{-48m\big[\frac{2}{\epsilon}-\log\Big(\frac{\Delta(\mu^2)}{\mu_D^2}\Big)-\gamma_E+\log(4\pi)-\frac{1}{2}\big]+\frac{2B\mu^2}{\Delta(\mu^2)}+\frac{8m^3}{\Delta(\mu^2)}\Big\}\ . \tag{E.64}$$

So we find, after some algebra to simplify the expression, that the renormalized three-point function is given by:

$$\frac{ig^3}{(4\pi)^2}\int_0^1 d\beta d\gamma\Big[\underbrace{48m\log\Big(\frac{\Delta(p^2)}{\Delta(\mu^2)}\Big)}_{1}+\underbrace{\frac{2p^2B}{\Delta(p^2)}-\frac{2\mu^2B}{\Delta(\mu^2)}}_{2}+\underbrace{8m^3\big(\frac{1}{\Delta(p^2)}-\frac{1}{\Delta(\mu^2)}\big)}_{3}\Big]-i\lambda_{3,R}\ . \tag{E.65}$$

We will check that each of these terms is suppressed. For the second term it is easy to see, as B depends on one power of m whereas Δ depends on m^2. The first term can be rewritten. We'll introduce the notation $\sigma\equiv(\beta+2\gamma)^2-\beta-4\gamma$ to keep the notation uncluttered. We then write:

$$48m\log\Big(\frac{\Delta(p^2)}{\Delta(\mu^2)}\Big)=48m\log\Big(\frac{\sigma p^2+m^2}{\sigma\mu^2+m^2}\Big)=48m\log\Big(\frac{m^2(1+\sigma p^2/m^2)}{m^2(1+\sigma\mu^2/m^2}\Big)\approx 48\big[\frac{\sigma(p^2-\mu^2)}{m}-\frac{\sigma^2(p^4-\mu^4)}{2m^3}+\dots\big]\ , \tag{E.66}$$

which is indeed suppressed with powers of m. The last term is rewritten as:

$$\begin{aligned}8m^3\big(\frac{1}{\Delta(p^2)}-\frac{1}{\Delta(\mu^2)}\big)&\approx 8m^3\Big[\frac{1}{m^2}(1-\frac{\sigma p^2}{m^2}+\frac{\sigma^2p^4}{m^4}-\dots)-\frac{1}{m^2}(1-\frac{\sigma\mu^2}{m^2}+\frac{\sigma^2\mu^4}{m^4}-\dots)\Big]=\\&=\frac{8\sigma(\mu^2-p^2)}{m}-\frac{8\sigma^2(\mu^4-p^4)}{m^3}+\dots\ ,\end{aligned} \tag{E.67}$$

which is also suppressed.

References

[1] P. Dirac, "The quantum theory of the emission and absorption of radiation .", Royal Society **114**, https://doi.org/10.1098/rspa.1927.0039 (1927).

[2] A. Wüthrich, "Feynman's Struggle and Dyson's Surprise: The Development and Early Application of a New Means of Representation. .", Traditions and Transformations in the History of Quantum Physics: Third International Conference on the History of Quantum Physics, Berlin, 10.34663/9783945561225-13 (2013).

[3] *The nobel prize in physics 1965*, https://www.nobelprize.org/prizes/physics/1965/summary/, Accessed: 21-07-2022.

[4] P. W. Higgs, "Broken Symmetries and the Masses of Gauge Bosons.", Physical Review Letters **13**, https://doi.org/10.1103/PhysRevLett.13.508 (1964).

[5] T. A. Collaboration, "Observation of a New Particle in the Search for the Standard Model Higgs Boson with the ATLAS Detector at the LHC .", Physics Letters B **716**, https://doi.org/10.1016/j.physletb.2012.08.020 (2012).

[6] G. Reijns, "The role of renormalization schemes in the context of the SM Hierarchy problem: Investigating the implications of a heavy quark model", MA thesis (Radboud University Nijmegen, the Netherlands, 2021).

[7] M. E. Peskin and D. V. Schroeder, *An introduction to quantum field theory* (CRC Press, 2019).

[8] W. Beenakker, *Reader for the course quantum field theory*, 2022.

[9] J. Ward, "An Identity in Quantum Electrodynamics.", Physical Review **78(2)**, 10.1103/PhysRev.78.182 (1950).

[10] M. Tanabashi et al., "Review of Particle Physics.", Phys. Rev. D. **98**, https://doi.org/10.1103/PhysRevD.98.030001 (2018).

[11] F. Englert and R. Brout, "Broken Symmetries and the Mass of Gauge Vector Mesons.", Physical Review Letters **13**, https://doi.org/10.1103/PhysRevLett.13.321 (1964).

[12] B. M. Schwarzschild, "Englert and Higgs are awarded the Nobel Prize in Physics.", Physics Today **66**, https://doi.org/10.1063/PT.3.2196 (2013).

[13] C. Collaboration, "Observation of a new boson at a mass of 125 GeV with the CMS experiment at the LHC.", Physics Letters B **716**, https://doi.org/10.1016/j.physletb.2012.08.021 (2012).

[14] G. 't Hooft and M. Veltman, "Regularization and Renormalization of Gauge Fields.", Nuclear Physics B **44**, https://doi.org/10.1016/0550-3213(72)90279-9 (1972).

[15] R. Kleiss, *Quantum field theory: a diagrammatic approach* (Cambridge University Press, 2021).

[16] N. Nakanishi, "General Theory of Infrared Divergence.", Progress of Theoretical Physics **19**, 159–169 (1958).

[17] T. Appelquist and J. Carazzone, "Infrared singularities and massive fields.", Physical Review D **11**, 10.1103/physrevd.11.2856 (1975).

[18] D. Skinner, *Quantum field theory ii: perturbative renormalization*, 2022.

[19] G. Burdman, *Quantum field theory ii: the callan-symanzik equation*, 2021.

[20] I. Brivio and M. Trott, "The Standard Model as an Effective Field Theory.", Phys.Rept. **793**, 10.1016/j.physrep.2018.11.002 (2019).

[21] W. Hollik and S. Paßehr, "Higgs boson masses and mixings in the complex MSSM with two-loop top-Yukawa-coupling corrections.", Journal of High energy Physics **10**, `https://doi.org/10.48550/arXiv.1409.1687` (2014).

[22] S. Mooij and M. Shaposhnikov, "Finite Callan-Symanzik renormalisation for multiple scalar fields.", JHEP, `https://doi.org/10.48550/arXiv.2110.15925` (2021).